Journal of the American Heart Association

ORIGINAL RESEARCH

Brain Kynurenine Pathway and Functional Outcome of Rats Resuscitated From Cardiac Arrest

Jacopo Lucchetti, MSc, PhD;* Francesca Fumagalli, MSc, PhD;* Davide Olivari, PhD; Roberta Affatato, PhD; Claudia Fracasso, MBiol; Daria De Giorgio, MBiol; Carlo Perego, BS; Francesca Motta, MBiol; Alice Passoni, MBiol; Lidia Staszewsky, MD; Deborah Novelli, PhD; Aurora Magliocca, MD, PhD; Silvio Garattini, MD; Roberto Latini, MD; Giuseppe Ristagno, MD, PhD; Marco Gobbi, PhD

BACKGROUND: Brain injury and neurological deficit are consequences of cardiac arrest (CA), leading to high morbidity and mortality. Peripheral activation of the kynurenine pathway (KP), the main catabolic route of tryptophan metabolized at first into kynurenine, predicts poor neurological outcome in patients resuscitated after out-of-hospital CA. Here, we investigated KP activation in hippocampus and plasma of rats resuscitated from CA, evaluating the effect of KP modulation in preventing CA-induced neurological deficit.

METHODS AND RESULTS: Early KP activation was first demonstrated in 28 rats subjected to electrically induced CA followed by cardiopulmonary resuscitation. Hippocampal levels of the neuroactive metabolites kynurenine, 3-hydroxy-anthranilic acid, and kynurenic acid were higher 2 hours after CA, as in plasma. Further, 36 rats were randomized to receive the inhibitor of the first step of KP, 1-methyl-DL-tryptophan, or vehicle, before CA. No differences were observed in hemodynamics and myocardial function. The CA-induced KP activation, sustained up to 96 hours in hippocampus (and plasma) of vehicle-treated rats, was counteracted by the inhibitor as indicated by lower hippocampal (and plasmatic) kynurenine/tryptophan ratio and kynurenine levels. 1-Methyl-DL-tryptophan reduced the CA-induced neurological deficits, with a significant correlation between the neurological score and the individual kynurenine levels, as well as the kynurenine/tryptophan ratio, in plasma and hippocampus.

CONCLUSIONS: These data demonstrate the CA-induced lasting activation of the first step of the KP in hippocampus, showing that this activation was involved in the evolving neurological deficit. The degree of peripheral activation of KP may predict neurological function after CA.

Key Words: cardiac arrest ■ cardiopulmonary resuscitation ■ indoleamine 2,3-deoxygenase ■ kynurenine pathway ■ neurological deficit

Mortality is high after cardiac arrest (CA) as a consequence of the "post-CA syndrome," a complex pathophysiological process following the return of spontaneous circulation (ROSC). It is characterized by myocardial dysfunction with circulatory shock, systemic inflammation with activation of the clotting system, and brain injury.[1]

Cardiovascular failure accounts for most deaths in the first 3 days after ROSC, while brain injury accounts for later deaths in two thirds of patients after out-of-hospital CA

Correspondence to: Giuseppe Ristagno, MD, PhD, Department of Pathophysiology and Transplantation, University of Milan, Milan, Italy.Department of Anesthesiology, Intensive Care and Emergency, Fondazione IRCCS Ca' Granda Ospedale Maggiore Policlinico, Via Francesco Sforza 35, 20122, Milan, Italy. E-mail. gristag@gmail.com

*J. Lucchetti and F. Fumagalli contributed equally.

Supplementary Material for this article is available at https://www.ahajournals.org/doi/suppl/10.1161/JAHA.121.021071

For Sources of Funding and Disclosures, see page 12.

JAHA is available at: www.ahajournals.org/journal/jaha

CLINICAL PERSPECTIVE

What Is New?

- Kynurenine pathway is an emerging key component of postcardiac arrest syndrome, affecting brain injury and survival after cardiac arrest.
- This study demonstrates early, prolonged activation of the kynurenine pathway in the blood and brain after successful resuscitation and its involvement in the evolving neurological deficits.

What Are the Clinical Implications?

- The study results point to new neuroprognostic biomarkers and therapeutic targets for cardiac arrest–induced brain injury.

Nonstandard Abbreviations and Acronyms

1-DL-MTRP	1-methyl-DL-tryptophan
3-HAA	3-hydroxyanthranilic acid
5-HT	5-hydroxytryptamine
Arg1	arginase 1
CA	cardiac arrest
IDO	indoleamine 2,3-dioxygenase
IL1β	interleukin 1 beta
NMDA	N-methyl-d-aspartate
KP	kynureninepathway
KYNA	kynurenic acid
NDS	neurological deficit score
PR	post–return to spontaneous circulation
RM	repeated measures
ROSC	return to spontaneous circulation

and in approximately a quarter of patients after in-hospital CA.[2] As many as 30% of CA survivors experience permanent brain damage, and as many as two thirds of resuscitated patients are discharged from hospital with variable degrees of neurological dysfunction[3] including seizures, myoclonus, memory impairment, cognitive dysfunction, fatigue, emotional behavior, posttraumatic stress symptoms, and difficulties in managing daily activities.[4–8]

Brain injury after CA is caused by the brain's vulnerability to the ischemic/reperfusion insult,[9] which leads to a complex cascade of cellular and molecular events, eg, activation of microglia and astrocytes, infiltration of circulating macrophages, excitotoxicity, cytokines release, disrupted calcium homeostasis, free radical formation, and pathological protease cascades,[1,10] exacerbating the ischemic/reperfusion injury. To predict the functional/neurological outcome a multimodal approach, which also includes the analysis of circulating biomarkers, is needed due to the complexity and interplay events occurring in the post-CA phase.[11–13] Thus, a better understanding of the underlying pathological molecular mechanisms is required to identify new, specific prognostic biomarkers and develop targeted therapeutic approaches.

The kynurenine pathway (KP) is emerging as one of the potential key components of brain injury after CA.[14] KP is the major pathway of catabolism of the essential amino-acid tryptophan, which is converted first into kynurenine (through the intermediate L-formylkynurenine) by the rate-limiting enzyme indoleamine 2,3-dioxygenase (IDO)[15,16] (the pathway is schematically shown in Figure S1). IDO is widely expressed in a variety of human tissues, as well as in circulating macrophages and dendritic cells, and is stimulated by proinflammatory cytokines, lipopolysaccharides, and free radicals.[17] KP activation has been described in various clinical conditions, including cardiovascular diseases,[18] cancer,[19] diabetes,[20] infections,[21] depression,[22] schizophrenia,[23] neurodegenerative disorders,[24] sepsis,[25,26] and after cardiac bypass and thoracic surgery.[27] We recently found early and prolonged activation of peripheral KP in patients resuscitated from out-of-hospital CA, related to the severity of post–CA shock, early death in the intensive care unit, and 12-month poor long-term outcome.[28] Activation of KP has also been implicated in situations causing neurological injury in patients in the intensive care unit[29] and in the adverse prognosis in patients with stroke[30] and trauma.[31]

Several downstream metabolites of kynurenine have important activities in the brain.[32] Some have neurotoxic/excitotoxic properties such as 3-hydroxyanthranilic acid (3-HAA) that auto-oxidize, leading to cerebral oxidative stress,[12] and quinolinic acid, which acts as a potent agonist of *N*-methyl-D-aspartate (NMDA) receptors.[32] The main neuroprotective metabolite is kynurenic acid (KYNA), which is an antagonist at NMDA receptors,[33,34] AMPA receptors,[35] alpha 7 nicotinic acetylcholine receptors,[36] and the aryl hydrocarbon receptor agonist.[37]

The present study investigated the activation of KP in CA-induced brain injury, measuring tryptophan for the first time and the KP metabolites kynurenine, KYNA, and 3-HAA directly in the hippocampus and in plasma of rats resuscitated from CA at different times post-ROSC. As proof of concept, we then checked the effect of the competitive IDO inhibitor, 1-methyl-DL-tryptophan (1-DL-MTRP), in preventing KP-induced neurological deficit in a more severe experimental model of CA.

METHODS

Data Availability

The data that support the findings of this study are available from the corresponding author upon reasonable request.

Animal Care

Procedures involving animals were conducted at the Istituto di Ricerche Farmacologiche Mario Negri IRCCS, which adheres to the principles set out in the following laws, regulations, and policies governing the care and use of laboratory animals: Italian Governing Law (D.lgs 26/2014; Authorisation n.19/2008-A issued March 6, 2008, by the Ministry of Health); Mario Negri Institutional Regulations and Policies providing internal authorization for persons conducting animal experiments (Quality Management System Certificate – UNI EN ISO 9001:2015 – Reg. N° 6121); the National Institutes of Health *Guide for the Care and Use of Laboratory Animals* (2011 edition), and EU directives and guidelines (EEC Council Directive 2010/63/UE). The study also followed the ARRIVE criteria.[38] A minimum of 9 rats per timing of measurements had been planned; the number of animals was reduced to a minimum necessary in order to be able to appreciate a significant difference of 50%, with a power of 0.8 and an error of probability of 0.05 (free software G*Power) taking into account the variability, in terms of KP metabolites levels, previously observed.[14]

Aim No. 1: Systemic and Central KP Activation After CA and Cardiopulmonary Resuscitation

The experimental design is illustrated in Figure 1A. The aim of this study was to investigate the systemic and central (ie, hippocampus) activation of the KP after CA followed by cardiopulmonary resuscitation (CA/CPR). In parallel, evaluation of the hemodynamic response was examined. A full description of the methods for animal preparation, CA/CPR procedure, and measurements are given in Data S1.

Animal Preparation

Male Sprague-Dawley ex-breeder rats (weight, 481±6 g; n=37) (Envigo) were used for the study. Thirty-two rats were anesthetized and instrumented for hemodynamic measurements and induction of CA, as previously reported.[39] CA/CPR was performed in 28 rats, while CA was not induced in 4 rats, which were included in the sham group. Five naive (nonoperated) rats were used as additional controls. Sham and naive rats were used for hippocampal analysis, as described in the Results section.

Experimental Procedures

We used an established model of electrically induced CA/CPR.[39] Briefly, animals were subjected to 7 minutes of untreated CA and 5 minutes of CPR, including mechanical chest compression, ventilation with oxygen, and defibrillation. Blood samples were serially collected from the femoral artery cannula in 3K-EDTA tubes 15 minutes before CA (pre-CA), and 10 minutes and 2 hours after ROSC. Rats were then euthanized with an intraperitoneal injection of pentobarbital sodium (150 mg/kg), and the brain was carefully removed, dissected to isolate hippocampal region, and immediately frozen in liquid N_2 before storage at –80 °C.

Measurements

Hemodynamics were recorded as previously described.[39] Briefly, ECG, aortic pressure, and right atrial pressure were continuously monitored for up to 2 hours after ROSC on a personal computer–based data acquisition system supported by CODAS hardware and software (DataQ). Coronary perfusion pressure was calculated in the same time range as the difference between time-coincident diastolic aortic and right atrial pressures.

Aim No. 2: Effect of IDO Inhibitor on CA-Induced KP Activation and Neurological Deficit

The experimental design is illustrated in Figure 1B. The aim of this study was to investigate whether pretreatment with 1-DL-MTRP, an inhibitor of the enzyme IDO-1, interferes with KP activation after CA/CPR and prevents neurological injury. A full description of the methods for animal preparation, CA/CPR procedure, and measurements are given in Data S1.

Animal Preparation and Pharmacological Treatment

Male Sprague-Dawley ex-breeder rats (weight, 480±5 g; n=42) (Envigo) were used. Six rats were used as naive controls and 36 were anesthetized and instrumented for hemodynamic measurements and induction of CA.[39] Before the induction of anesthesia, the 36 rats were randomized using no transparent envelopes and assigned into 2 experimental groups:

1. Treatment group (1-DL-MTRP, n=17), receiving 2 equal doses of the IDO inhibitor 1-DL-MTRP by gavage, 16 and 2 hours before CA; 1-D-MTRP (Sigma Aldrich Italia) and 1-L-MTRP (Sigma Aldrich Italia) were dissolved in 1% carboxymethylcellulose and given orally by gavage to a final dose of 800 mg/kg of racemate.
2. Control group (vehicle, n=19), receiving an equal volume of 1% carboxymethylcellulose in deionized water by gavage, 16 and 2 hours before CA.

Experimental Procedures

Animals were subjected to 8 minutes of untreated CA and 8 minutes of CPR, including mechanical chest

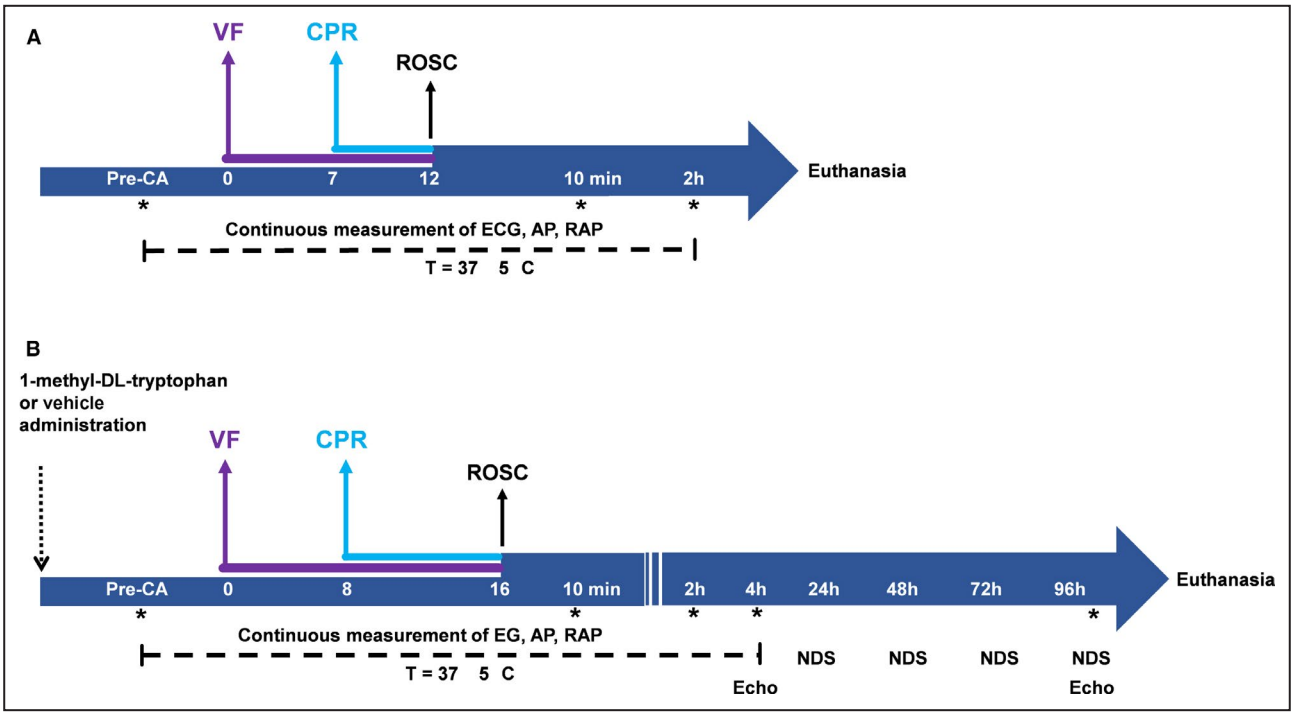

Figure 1. Experimental designs.
Experimental designs adopted for (**A**) aim no. 1 and (**B**) aim no. 2. *Blood (0.6 mL) drawn for measurement of plasma 1-methyl-DL-tryptophan, kynurenine pathway metabolites, and plasma high-sensitivity cardiac troponin T. BL=baseline (before cardiac arrest [pre-CA]). AP indicates arterial pressure; CPR, cardiopulmonary resuscitation; Echo, transthoracic echocardiography; NDS, neurological deficit score; RAP, right atrial pressure; ROSC, return of spontaneous circulation; and VF, ventricular fibrillation.

compression, ventilation with oxygen, and defibrillation. This is a longer and more severe CA experimental model than that used for aim no. 1, with the intent to exacerbate KP activation. The CA/CPR procedure was performed by investigators blinded to the 2 experimental groups. Four hours after ROSC, all of the catheters and the endotracheal tubes were removed. The animals were returned to their cages and were observed up to 96 hours after resuscitation. Animals were given ampicillin (50 mg/kg intramuscular) and buprenorphine (0.16 mg/kg) to prevent infection and pain. Blood samples were serially collected from the femoral artery cannula in 3K-EDTA tubes 15 minutes pre-CA, and 2 and 96 hours post-ROSC (PR 2 hours and PR 96 hours). At 96 hours, rats were euthanized with an intraperitoneal injection of pentobarbital sodium (150 mg/kg), and the brain was removed, dissected to isolate hippocampus and cortex, and immediately frozen in liquid N_2 before storage at −80 °C.

Measurements

ECG, aortic pressure, and right atrial pressure were continuously monitored for up to 4 hours post-ROSC, as described for aim no. 1. Myocardial function was assessed at 4 and 96 hours post-ROSC by transthoracic monodimensional, bidimensional, pulse, color, and tissue Doppler echocardiography (Aloka SSD-5500). Left ventricular ejection fraction and the septum mitral inflow ratio (ie, the ratio of the early transmitral pulsed Doppler inflow velocity to peak early diastolic mitral annulus velocity by tissue Doppler) were measured and calculated to evaluate LV systolic and diastolic function, respectively. For echocardiographic analysis at 96 hours, rats were anesthetized with intraperitoneal thiopental 50 mg/kg and, if necessary, 10 mg/kg recall doses. Plasma high-sensitivity cardiac troponin T (hs-cTnT) concentration was assayed at pre-CA and 4 and 96 hours post-ROSC with an electrochemiluminiscence assay (ECLIA, Elecsys 2010 analyzer; Roche Diagnostics) following manufacture instructions.

Neurological Assessment

Neurological deficit score (NDS)[39] was used to assess neurologic recovery 24, 48, 72, and 96 hours post-ROSC. In brief, the test, ranging from 0 (normal) to 500 (brain death), rated level of consciousness, respiration, motor and sensory functions, and overall behavior. The score was decided by collaborators blinded to the study groups.

Inflammatory Gene Expression

Total RNA was extracted form brain cortex with a commercial kit (Pure Link RNA Mini Kit, Ambion) and

processed for real-time reverse transcription polymerase chain reaction analysis of gene expression levels for *interleukin 1 beta (IL1β) and Arginase 1 (Arg1). Glyceraldehyde 3-phosphate dehydrogenase (Gapdh)* was used as the reference gene, and primer sets were designed to span exon junctions (https://www.ncbi.nlm.nih.gov/tools/primer-blast/).

KP Metabolites and Serotonin Measurements in Plasma and Hippocampus by High-Performance Liquid Chromatography-Tandem Mass Spectrometry

Blood samples were centrifuged at 2000*g* for 15 minutes at 4 °C and plasma was stored at −80 °C until analysis. On the day of analysis, hippocampi were thawed, accurately weighed, and homogenized in 5 volumes of H_2O/acetonitrile (1:2, v/v). Plasma and hippocampal levels of 1-DL-MTRP (aim no. 2), tryptophan (aims no. 1 and no. 2) and its metabolites, kynurenine (aims no. 1 and no. 2), KYNA (aim no. 1), 3-HAA (aim no. 1), and 5-hydroxytryptamine (5-HT; aim no. 2 in hippocampus) were measured using high-performance liquid chromatography coupled with tandem mass spectrometry. Briefly, deuterated internal standards were added to plasma and hippocampal homogenate; plasma samples were then mixed with cold methanol and incubated at −20 °C for protein precipitation before centrifugation; an appropriate volume of hippocampal homogenate was centrifuged directly. After centrifugation, supernatant was dried under N_2 and the residue was resuspended and injected into the high-performance liquid chromatography system. Separation was performed following a gradient elution and mass spectrometric analysis was done with a triple quadrupole mass spectrometer in positive ion mode and multiple reaction monitoring mode, measuring the fragmentation products of the deprotonated pseudomolecular ions. A full description of the high-performance liquid chromatography coupled with tandem mass spectrometry methods used for aims no. 1 and no. 2 is given in Data S1.

Statistical Analysis

The GraphPad Prism program (GraphPad Software) was used for data processing and statistical analysis. A 1-sample Kolmogorov–Smirnov *Z* normality test was used to inspect normal distribution of the data. Continuous variables were analyzed by 1-way repeated-measures (RM) ANOVA followed by Tukey multicomparison test for normally distributed data; non-normally distributed data were analyzed with Kruskal-Wallis test (for non-RM) or Friedman test (for RM) followed by Dunn multicomparison test. *T* test or Mann-Whitney *U* test (2-tailed *P* value, 95% CI), respectively, was used for comparison between 2 groups of normally and non-normally distributed data. Two-way ANOVA followed by Sidak multiple comparisons test was used: variables non-normally distributed were corrected by logarithmic (natural log) transformation before 2-way ANOVA with Sidak multiple comparisons test. Ordinary (non-RM) or RM 2-way ANOVA were used when appropriate, as reported in the legends of the figures and tables.

When the dependent variable was categorical, Fisher exact test was used. Spearman rank correlation coefficient was used to analyze correlations between variables. $P<0.05$ was considered significant.

RESULTS

Aim no. 1: Survival and Resuscitation Outcome

CA was induced in 28 rats, 23 of which (82%) were successfully resuscitated. Table S1 reports hemodynamic variables and plasma levels of hs-cTnT.

Each rat developed marked post-ROSC hemodynamic instability during the 2-hour observation, as expected. Heart rate was significantly reduced 10 minutes post-ROSC compared with baseline ($P<0.0001$ versus pre-CA) then returned to pre-CA values (Table S1). Systolic atrial pressure, mean arterial pressure, diastolic arterial pressure, and coronary perfusion pressure remained low for 2 hours post-ROSC ($P<0.0001$, Table S1).

Circulating levels of hs-cTnT reflected the development of postresuscitation myocardial injury. Median plasma levels of hs-cTnT were significantly higher at 10 minutes ($P<0.0001$) and 2 hours ($P=0.0002$) post-ROSC compared with pre-CA levels (Table S1).

Aim no. 1: CA/CPR Alters KP Metabolites Levels in Plasma and Hippocampus

The effect of CA on plasma tryptophan and kynurenines is reported in Table 1. Ten-minute post-ROSC tryptophan levels were 12% lower ($P=0.0059$) and kynurenine levels were 36% higher ($P=0.0001$). The early activation of the tryptophan→kynurenine step of the KP is highlighted by the significant increases of the kynurenine/tryptophan ratio ($P<0.0001$). Regarding downstream KP metabolites, KYNA levels showed a 5-fold increment ($P<0.0001$), while 3-HAA levels decreased slightly but not significantly. Two hours post-ROSC, kynurenine levels were still higher than pre-CA ($P=0.0012$), suggesting that the tryptophan→kynurenine step remained activated (1.3-fold increase of kynurenine/tryptophan ratio, $P=0.0007$ versus pre-CA). At the same time, KYNA levels were still high ($P=0.0035$ versus

Table 1. Plasma and hippocampal KP activation after CA/CPR

Plasma		Hippocampus	
Metabolite	**Median [quartile 1–quartile 3]**	**Metabolite**	**Median [quartile 1–quartile 3]**
Tryptophan, μg/mL		Tryptophan, μg/g	
Pre-CA	17.00 [13.95–20.63]	Controls	5.05 [4.80–5.20]
PR 10 min	14.65 [13.00–18.05]*		
PR 2 h	15.59 [13.73–16.87]	PR 2 h	8.09 [7.60–8.98]‖
Kynurenine, μg/mL		Kynurenine, μg/g	
Pre-CA	0.561 [0.374–0.690]	Controls	0.052 [0.042–0.076]
PR 10 min	0.704 [0.541–0.957]†		
PR 2 h	0.700 [0.493–0.886]†	PR 2 h	0.134 [0.096–0.169]‖
Kynurenine/tryptophan ratio		Kynurenine/tryptophan ratio	
Pre-CA	0.030 [0.023–0.040]		
PR 10 min	0.051 [0.039–0.061]†	Controls	0.011 [0.009–0.015]
PR 2 h	0.044 [0.036–0.065]†	PR 2 h	0.015 [0.013–0.020]$
KYNA, ng/mL		KYNA, ng/g	
Pre-CA	10.04 [7.92–4.77]	Controls	2.43 [2.08–3.25]
PR 10 min	57.03 [39.16–116.2]†		
PR 2 h	17.80 [11.18–40.43]†	PR 2 h	6.95 [5.75–10.83]‖
3-HAA, ng/mL		3-HAA, ng/g	
Pre-CA	2.137 [1.733–2.526]	Controls	0.222 [0.177–0.239]
PR 10 min	1.780 [0.962–2.227]		
PR 2 h	2.762 [1.667–3.532]‡	PR 2 h	0.301 [0.276–0.545]‖

Plasma concentrations of tryptophan, kynurenine, the kynurenine/tryptophan ratio, kynurenic acid (KYNA), and 3-hydroxyanthranilic acid (3-HAA) were measured in operated rats before cardiac arrest (pre-CA) and 10 minutes and 2 hours post–return to spontaneous circulation (PR 10 minutes and PR 2 hours) (n=23 rats). For hippocampal analysis, tryptophan and kynurenine pathway (KP) metabolites were measured in naive rats (n=5) and in sham-operated rats (n=4) and 2 hours PR (2 hours, n=23). Since there were no statistical differences between naive and sham rats (absolute levels and statistical analysis are reported in Table S2), these data were pooled as a control group (n=9) to evaluate the effect of cardiac arrest (CA). Effect of CA: absolute plasma levels were analysed with Friedman test for repeated measures, followed by Dunn multiple comparisons post hoc test, *P<0.01 and †P<0.001 vs pre-CA; ‡P<0.01 vs PR 10 minutes; absolute hippocampal levels were analyzed with Mann-Whitney U test for nonrepeated measures: $$P$<0.05 and ‖$P$<0.001 vs controls. Exact P values for each comparison are reported in the text. CPR indicates cardiopulmonary resuscitation.

pre-CA), although with a tendency to decrease from the 10-minute post-ROSC values (P=0.0550).

KP values were preliminarily analyzed in the hippocampus of naive and sham rats (Table S2). Hippocampal levels of tryptophan and kynurenines metabolites were not significantly altered by surgical procedures alone (anesthesia and instrumentation as described in the Methods section); naive and sham rats were therefore pooled and considered as controls for subsequent analyses. Two hours post-ROSC, hippocampal tryptophan levels had risen 60% (P<0.0001), in contrast with the decrease in plasma. The effect of CA on hippocampal kynurenine levels was even greater (+159%, P<0.0001), with an increase of the kynurenine/tryptophan ratio (+36%, P=0.0145). Median KYNA and 3-HAA levels also increased by 186% (P=0.0001) and 36% (P<0.0001), respectively.

Aim no. 2: Effect of IDO Inhibition

The 2 oral doses of 800 mg/kg of 1-DL-MTRP given 16 and 2 hours before CA resulted in similar plasma concentrations at 15 minutes pre-CA and 2 hours post-ROSC, with an average of 34 μg/mL (range, 20–40 μg/mL), which declined slightly to 21 μg/mL on average 96 hours post-ROSC (Figure S2A). At this last time, hippocampal concentrations of the drug were 11.4 μg/g on average (Figure S2B), with a tissue-to-plasma ratio of ≈0.54.

Effects on Survival, Hemodynamic, and Myocardial Function

Treatment with 1-DL-MTRP had no effect on body weight, heart rate, hemodynamics, or circulating biomarkers in the 2 groups pre-CA (Table 2). There were no differences in coronary perfusion pressure during CPR (Table 2), reflecting adequate standard chest compression quality in both groups. The duration of CPR and the number of defibrillations delivered to achieve ROSC were lower in animals treated with 1-DL-MTRP than those given vehicle; however, these differences were not statistically significant (Table 2). Pretreatment with 1-DL-MTRP had no effect on the number of successfully resuscitated animals (1-DL-MTRP 88%, vehicle 84%) and

Table 2. CPR Outcomes, Hemodynamics, and Myocardial Functions in CA/CPR Rats Treated With 1-DL-MTRP

Outcomes	Vehicle (n=19)	1-DL-MTRP (n=17)
Body weight, g	480±24	481±25
Resuscitation, no./total	16/19	15/17
Time to ROSC, s	481 [478–482]	481 [370–482]
Shocks to ROSC, no.	1	1
4-h survival, no./resuscitated	16/16	15/15
96-h survival, no./ resuscitated	10/16	10/15
CPP, mm Hg		
Pre-CA	111±18	109±13
PR 10 min	44±17	57±21
PR 1 h	76±12	84±9
PR 2 h	71±14	81±12
PR 3 h	71±18	75±15
PR 4 h	71±17	73±20
HR, beats per min		
Pre-CA	368±34	375±34
PR 10 min	194±57	237±54*
PR 1 h	335±37	335±12
PR 2 h	338±36	360±20
PR 3 h	350±26	358±23
PR 4 h	352±33	351±51
SAP, mm Hg		
Pre-CA	152±9	151±13
PR 10 min	88±20	103±17*
PR 1 h	111±12	117±9
PR 2 h	110±15	118±12
PR 3 h	107±14	111±18
PR 4 h	106±11	115±17
DAP, mm Hg		
Pre-CA	118±10	114±12
PR 10 min	44±17	57±21
PR 1 h	77±13	84±9
PR 2 h	72±15	81±12
PR 3 h	70±18	74±15
PR 4 h	70±16	78±15
MAP, mm Hg		
Pre-CA	127±12	127±13
PR 10 min	59±19	76±20*
PR 1 h	95±30	96±9
PR 2 h	86±15	96±13
PR 3 h	83±16	89±16
PR 4 h	83±16	94±17
LVEF, %		
PR 4 h	33.6±3.6	36.8±3.2
PR 96 h	75.1±3.2	75.3±3.2
E/e' ratio		
PR 4 h	14.9±1.0	16.4±1.4
PR 96 h	15.9±2.6	16.2±1.3
hs-cTnT, pg/mL		
Pre-CA	100 [71–190]	98 [66–111]
PR 4 h	5995 [4942–9604]	4965 [2978–5242]
PR 96 h	64 [51–82]	64 [36–278]

Body weight (normal), resuscitation outcomes (non-normal), and survival rate (Fisher test). Hemodynamic parameters (normal) and myocardial functions were recorded up to 4 and 96 hours post–return of spontaneous circulation (PR), respectively. All data are shown as mean±SD when normally distributed or median [quartile 1–quartile 3] when non-normally distributed and analyzed by ordinary (for left ventricular ejection fraction [LVEF], septum mitral inflow (E/e'), and plasma high-sensitivity cardiac troponin T [hs-cTnT]) or repeated measures (for coronary perfusion pressure [CPP], heart rate [HR], systolic arterial pressure [SAP], diastolic arterial pressure [DAP], and mean arterial pressure [MAP]) 2-way ANOVA followed by Sidak multicomparison post hoc test, *P<0.05 vs time-matched vehicle-treated rats (effect of 1-methyl-DL-tryptophan [1-DL-MTRP]). Time and shock to return of spontaneous circulation (ROSC) were analyzed by the Mann-Whitney U test. CA indicates cardiac arrest; and CPR, cardiopulmonary resuscitation.

that survived up to 96 hours after CA (1-DL-MTRP 66%, vehicle 62%).

After resuscitation, animals treated with 1-DL-MTRP had higher systolic and mean diastolic pressures and coronary perfusion pressure compared with vehicle; systolic arterial pressure and mean arterial pressure were significantly higher 10 minutes post-ROSC (PR 10 minutes) and coronary perfusion pressure was markedly higher 2 hours after resuscitation in the 1-DL-MTRP–treated group compared with the vehicle-treated group. At 4 hours post-ROSC (PR 4 hours) in both study groups, left ventricular ejection fraction was severely compromised (normal reference value, 87.0%±1.7%) and septum mitral inflow ratio was slightly high (normal reference value, 12.0±0.9). At 96 hours post-ROSC (PR 96 hours), left ventricular ejection fraction returned to normal in both groups and the septum mitral inflow ratio did not change. There were no significant differences in plasma levels of hs-cTnT in the vehicle- and 1-DL-MTRP–treated groups (Table 2).

Effect on CA/CPR-Induced KP Activation

Fifteen minutes pre-CA, tryptophan levels in plasma of 1-DL-MTRP–treated rats were 27% higher than in vehicle-treated rats (P=0.0263), while kynurenine levels were 24% lower (P=0.0243). The kynurenine/tryptophan ratio therefore decreased 40% (P=0.0056) (Table S3). These data indicate inhibition of peripheral IDO activity by 1-DL-MTRP before CA.

In vehicle-treated rats, we confirmed early CA-induced peripheral KP activation (Figure 2), ie, a significant decrease in tryptophan plasma levels (22%, P=0.0444) and a significant increase in kynurenine plasma levels (33%, P=0.0461) 2 hours post-ROSC (PR

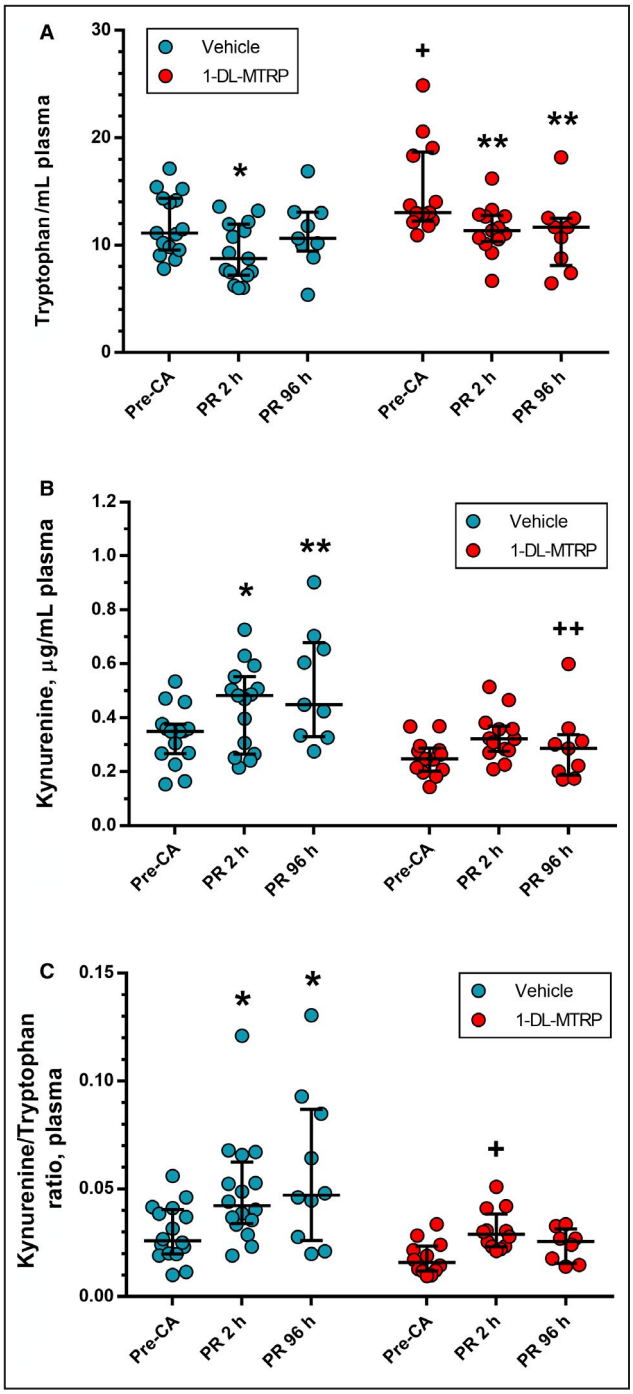

Figure 2. Indoleamine 2,3-dioxygenase inhibition counteracts cardiac arrest/cardiopulmonary resuscitation (CA/CPR)– induced kynurenine pathway (KP) activation in plasma.

Plasma levels of (**A**) tryptophan, (**B**) kynurenine, and **(C)** kynurenine/tryptophan ratio 15 minutes before cardiac arrest (pre-CA; n=13–15), 2 hours post–return of spontaneous circulation (PR; PR 2 hours [n=13–15]), and 96 hours PR (n=9) in vehicle- and 1-methyl-DL-tryptophan (1-DL-MTRP)–treated rats. Box plots show median, quartile range, and minumim–maximum range. Statistical analysis was performed on absolute values (pre-CA, PR 2 hours, and PR 96 hours) by ordinary 2-way ANOVA, followed by Sidak multiple comparisons post hoc test. $^{*}P<0.05$ and $^{**}P<0.01$ vs corresponding pre-CA levels (effect of CA). $^{+}P<0.05$ and $^{++}P<0.01$ vs time-matched vehicle-treated rats (effect of 1-DL-MTRP pretreatment).

2 hours). At 96 hours post-ROSC, tryptophan levels returned to pre-CA levels (Figure 2A), but kynurenine was still increased (+56%, P=0.0022) (Figure 2B). The kynurenine/tryptophan ratio was higher at 2 hours (+68%, P=0.0128) and 96 hours post-ROSC (+80%, P=0.0106) (Figure 2C).

In 1-DL-MTRP–treated rats, we found much lower effects of CA. In particular, following CA, plasma kynurenine levels and kynurenine/tryptophan ratio showed a slight, nonsignificant increase in comparison to pre-CA conditions, and, most important, they were markedly lower than in vehicle-treated rats at the same time points (Figure 2).

Hippocampal kynurenine levels of vehicle-treated rats were 109% higher than in naive rats (P=0.0064) 96 hours post-ROSC, resulting in a higher kynurenine/tryptophan ratio (+57%, P=0.0204) and indicating sustained activation of central KP (Figure). Kynurenine levels in 1-DL-MTRP–treated rats were significantly lower than in vehicle-treated rats (P=0.0409) and comparable to those in naive rats, resulting in a lower kynurenine/tryptophan ratio (P=0.0249) than for the vehicle-treated group) (Figure 3).

An important finding is that 96 hours post-ROSC, hippocampal levels of tryptophan, kynurenine, and the kynurenine/tryptophan ratio positively correlated with the levels of the same analytes in plasma (Figure 4), both in vehicle- and 1-DL-MTRP–treated rats.

In the same rats we also found that hippocampal 5-HT concentrations in vehicle- and 1-DL-MTRP–treated rats were superimposable to those measured in naive rats (Figure S3 and Table S4).

Effect on Neurological Functions and Central Inflammatory Response

Figure 5A reports the NDS measured 24, 48, 72, and 96 hours post-ROSC in rats pretreated with vehicle or 1-DL-MTRP. NDS values were lower in resuscitated rats pretreated with the IDO inhibitor than vehicle-treated rats, at all time points.

We found a significant positive correlation between the severity of the neurological deficit (96 hours post-ROSC in vehicle- and 1-DL-MTRP–treated rats) and kynurenine hippocampal levels (Figure 5B), as well as the kynurenine/tryptophan ratio (Figure 5C). Positive correlations were also found between NDS and plasma kynurenine levels (Figure 5D) and the kynurenine/tryptophan ratio (Figure 5E).

Further, hippocampal levels of 5-HT did not correlate with the NDS measured 96 hours post-ROSC (data not shown).

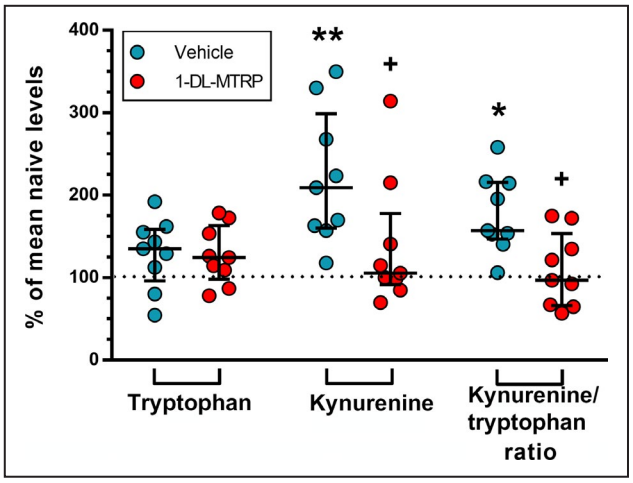

Figure 3. Indoleamine 2,3-dioxygenase inhibition counteracts CA/CPR–induced kynurenine pathway activation in hippocampus.
Concentrations of tryptophan, kynurenine, and the kynurenine/tryptophan ratio measured in hippocampus 96 hours post–return of spontaneous circulation (96 hours) in rats treated with vehicle (n=9) or 2 doses of 800 mg/kg 1-methyl-DL-tryptophan (1-DL-MTRP) given by gavage 16 and 2 hours before CA (n=9). Since this experiment included 2 independent sessions, each 1 including 3 naive rats, for each session we normalized tryptophan, kynurenine, and the kynurenine/tryptophan ratio in vehicle- and 1-DL-MTRP–treated rats to the means for the corresponding naive rats (absolute levels are reported in Table S4). Box plots show median, quartile range, and minimum–maximum range. Data were analyzed by Kruskal-Wallis test followed by Dunn multicomparison test. *P<0.05 and **P<0.01 vs naive. +P<0.05 vs vehicle time-matched. Exact P values are reported in the text.

We then examined inflammatory gene expression by real-time reverse transcription polymerase chain reaction in the brain cortex 96 hours post-ROSC (Figure S5). No statistically significant differences have been observed, although there was a tendency in the upregulation of IL1β and Arg1 after CA/CPR. Pretreatment with 1-DL-MTRP slightly reduced CA-induced IL1β upregulation, with a tendency towards an increase in Arg1 gene expression.

DISCUSSION

In this study we show that: (1) CA-induced activation of the KP, previously observed in plasma from animal models and humans and confirmed here in rats, is accompanied by parallel increases of KP metabolites in the hippocampus; (2) the increase of kynurenine, the metabolite resulting from IDO-mediated tryptophan conversion, is long-lasting and still present 96 hours after CA in plasma and hippocampus; (3) CA induces a clear neurological deficit in rats, which is counteracted by inhibition of IDO, suggesting the involvement of KP, which is further supported by (4) the positive correlation between neurological deficit and hippocampal

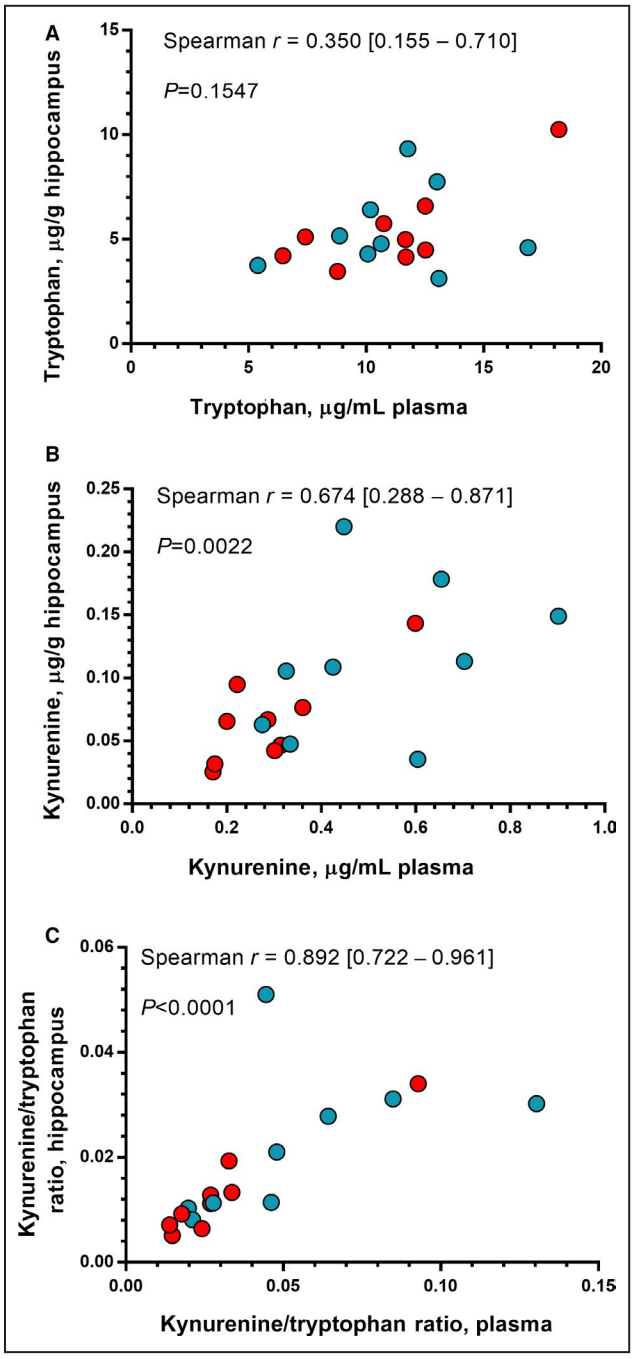

Figure 4. Hippocampal kynurenine pathway metabolites levels positively correlate with those in plasma.
Correlations between hippocampal levels of (**A**) tryptophan, (**B**) kynurenine, and (**C**) the kynurenine/tryptophan ratio 96 hours post–return of spontaneous circulation in vehicle- (teal blue circles, n=9) and 1-methyl-DL-tryptophan–treated rats (red circles, n=9). Correlations were calculated by Spearman method: rank correlation coefficient *r* [95% CI] and *P* value (2-tailed) of the correlations are indicated inside the figures. *P*<0.05 was considered significant.

kynurenine levels; and (5) the positive correlation between neurological deficit and plasma kynurenine levels also suggests that peripheral activation of KP is a marker of the functional status of the brain.

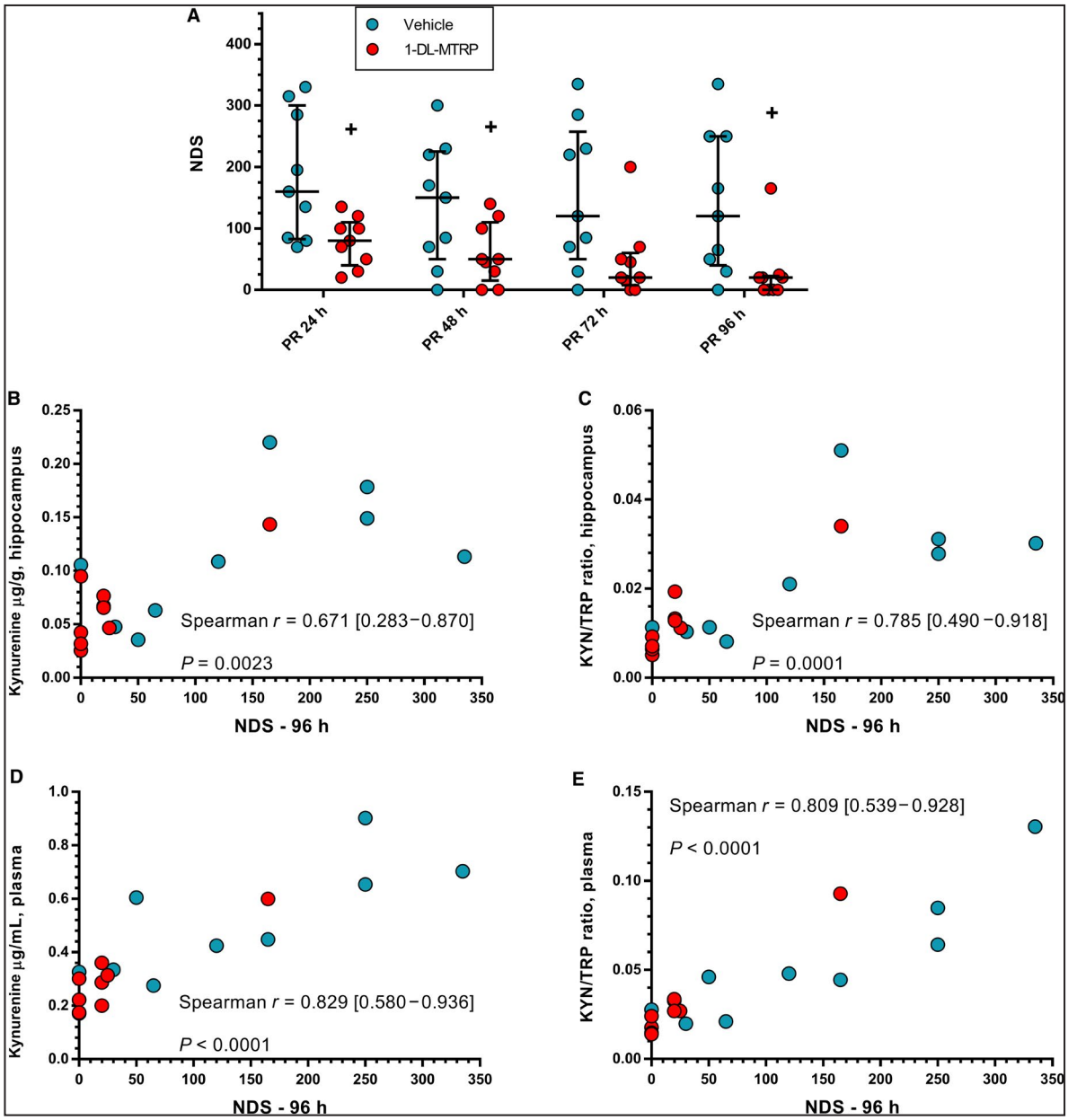

Figure 5. Time course of the neurological deficit score (NDS) after CA/CPR and correlation with hippocampal and plasmatic levels of kynurenine pathway metabolites.

A, NDS was calculated 24, 48, 72, and 96 hours post–return of spontaneous circulation (PR; PR 24 hours, PR 48 hours, PR 72 hours, and PR 96 hours) in rats treated by gavage 16 and 2 hours before CA with vehicle (n=9) or 1-methyl-DL-tryptophan (1-DL-MTRP; 800 mg/kg per dose [n=9]). Box plots show median, quartile range, and minimum–maximum range. Data were analyzed by 2-way repeated measures ANOVA, followed by Sidak multiple comparisons post hoc test. $^{+}P<0.05$ vs time-matched vehicle-treated rats. Panels **B-E** show correlations between NDS and hippocampal (**B** and **C**) and plasmatic (**D** and **E**) levels of kynurenine and the kynurenine/tryptophan ratio 96 hours PR in vehicle- (teal blue circles) and 1-DL-MTRP–treated rats (red circles). Correlations were calculated by Spearman method: rank correlation coefficient *r* [95% CI] and *P* value (2-tailed) of the correlation are indicated inside the figures. $P<0.05$ was considered significant. Correlations analysis between tryptophan, in plasma and hippocampus, and NDS are reported in Figure S4.

In the first experiment, we find in the plasma of a large number of rats, early (as soon as 10 minutes) and prolonged (up to 96 hours) activation of the first step of the KP (Table 1 and Figure 2) is most likely caused by IDO activation induced by the peripheral inflammatory and immune response after CA/CPR.[14,17,40–43] We also document for the first time a rapid (10 minutes) and marked (5-fold) increase of the downstream KP

metabolite KYNA, but not of 3-HAA, with a partial return toward pre-CA levels at 2 hours. The increase of circulating KYNA has been associated with anti-inflammatory[44,45] and antioxidative activities.[46] These results confirm and extend previous data in small and large animals, as well as humans, after CA/CPR.[14,28,47] A similar CA-induced alteration of peripheral KP metabolites between rats and humans has also recently been confirmed with a different rat model of CA,[48] thus supporting the use of rats as a suitable model for studying human CA.

We also analyzed, for the first time, the effect of CA on KP metabolites in the rat hippocampus, the brain region mainly affected by ischemic/reperfusion injury after successful resuscitation after CA, in humans[49,50] and animal models.[14,51,52] At variance with the results in plasma, hippocampal tryptophan concentrations were higher 2 hours post-ROSC (+69%), returning to pre-CA levels after 96 hours (Table 1 and Figure 3). Since tryptophan is an essential aminoacid, the rise in hippocampal levels after CA/CPR may be associated with an increase in blood-to-brain passage. Circulating tryptophan crosses the blood-brain-barrier in the free form through the large neutral amino acid transporter L-type amino acid transporter 1.[53] Therefore, the higher hippocampal tryptophan levels after CA/CPR might be attributable to CA-induced regional blood-brain-barrier breakdown[54–56] that facilitate the influx of the brain-permeable metabolites[32,57] and also of circulating macrophage infiltration,[32,58,59] thus increasing the influx of peripheral tryptophan. CA/CPR also markedly raised hippocampal kynurenine levels by 167% and 109% at 2 and 96 hours post-ROSC, respectively (Table 1 and Figure 3). Rodent studies suggest that ≈60% of brain kynurenine comes from peripheral sources[60] through the same mechanisms as tryptophan[53,61]; therefore, the increase in hippocampal kynurenine absolute levels may be caused by higher influx into the CNS as for tryptophan. However, considering that the CA-induced increase of hippocampal tryptophan dropped from 2 and 96 hours post-ROSC (69% and 10%, respectively), whereas in the same period the kynurenine/tryptophan ratio rose (36% and 57%), it follows that central IDO is most likely activated after CA/CPR.

The activation of the first step of the KP in the hippocampus also caused perturbation of the neuroactive KP downstream metabolites, and hippocampal KYNA (neuroprotective) and 3-HAA (neurotoxic) concentrations also rose 2 hours post-ROSC. The changes in KP metabolites levels might be ascribed to fluctuations in the activity of downstream KP enzymes caused by the proliferation/activation of resident microglia and astrocytes.[32,62–67] After CA/CPR, the neuroinflammatory response following brain hypoxia and reperfusion is also orchestrated by activated glial cells.[14,68–72] The changes in the neuroglial population might lead to unbalance in the downstream KP metabolites since the enzymatic steps kynurenine→KYNA and kynurenine→3-HAA (Figure S1) are physically segregated into 2 distinct cellular branches. Finally metabolized to quinolinic acid, 3-HAA is synthetized in the microglia, while kynurenine is converted to KYNA in astrocytes.[32,73–75]

The activation of the first step of the KP and the fluctuations in the levels of KYNA and 3-HAA suggest a perturbation of the whole pathway, with changes in the hippocampal levels of the other neuroactive metabolites. Higher levels of 3-HAA are generally associated with higher levels of quinolinic acid, which in addition to its activity as a potent agonist of the NMDA receptor,[76] also raises the levels of reactive oxygen and nitrogen species, stimulates lipid peroxidation, and causes mitochondrial dysfunctions.[32,77] It is also involved in deregulation of the phosphorylation state of several cellular proteins.[78,79]

We then confirm the involvement of KP activation on the central consequences of CA, assessed on the basis of the NDS at different times after ROSC. Our approach was to prevent the first step of KP, pretreating rats with 1-DL-MTRP, a well-known IDO inhibitor.[80–82] We used the dose of 800 mg/kg, since previous studies in animal models (rats and dogs) showed no further increase in the plasma concentration of 1-DL-MTRP with higher oral doses, because of saturable absorption and the absence of toxicity.[83] 1-DL-MTRP plasma levels after 2 oral doses 16 hours and 2 hours before CA confirmed the attainment of steady-state and slow elimination from blood.[83,84] Plasma and brain levels were, respectively, 21 µg/mL and 11.4 µg/g 96 hours post-ROSC, indicating good brain penetration of the inhibitor, in line with previous data.[83,84] These drug levels, corresponding to concentrations in the high micromolar range (52–96 µmol/L), are compatible with inhibition of the enzyme, since in vitro studies showed a *Ki* of 34 µmol/L.[80,81]

Pretreatment with 1-DL-MTRP therefore significantly lowered plasma levels of kynurenine and of the kynurenine/tryptophan ratio, indicating successful inhibition of the first step of KP. In these conditions, we observed significant improvement of the neurological function after CA,[85] in agreement with our hypothesis of involvement of the KP in the central events leading to brain injury after CA/CPR. Preclinical and clinical studies in stroke have in fact shown that interfering with the KP may have beneficial effects in terms of neuroprotection and reduction of neuroinflammation, lessening patient morbidity and mortality.[86] Our data indicate that pretreatment with 1-DL-MTRP reduced kynurenine levels in plasma and hippocampus 96 hours post-ROSC, and, consequently, the kynurenine/tryptophan ratio.

To investigate the effect of IDO inhibition on the hypoxic ischemic brain environment, we analyzed gene expression of factors associated with proinflammatory states and anti-inflammatory states, IL-1β, and Arg1, respectively.[87–89] The results are not conclusive but are suggestive for indicating an effect of 1-DL-MTRP in counteracting the CA/CPR-induced increase of IL-1β mRNA and in increasing Arg1 mRNA.

We did not find effects of CA/CPR on hippocampal 5-HT levels, a possible consequence of the shift toward the KP induced by IDO activation (Figure S3), nor were changes observed after treatment with 1-DL-MTRP. However, these measurements were performed 96 hours after ROSC, and it cannot be excluded that 5-HT alterations might occur at earlier time points. Moreover, the rapid turnover of 5-HT to form its downstream metabolites (eg, 5-hydroxyindoleacetic acid) could mask the effect of CA/CPR or IDO inhibition on central 5-HT levels.

Interestingly, despite interindividual variability in kynurenine levels and consequently in the kynurenine/tryptophan ratio after CA/CPR, we found significant correlations between individual kynurenine absolute levels, as well as kynurenine/tryptophan ratio and CA-induced neurological scores. These correlations were observed in hippocampal and plasma levels, suggesting that peripheral activation of KP may be a marker of functional outcome, consistent with previous findings in out-of-hospital CA patients[28] and in patients after stroke, where peripheral activation of the KP correlated with stroke severity and cerebral infarct volume.[30,90] Moreover, the correlation between plasma and hippocampal levels of kynurenine and kynurenine/tryptophan ratio also suggest that peripheral KP may reflect the situation in the brain.

In this study, we did not measure the hippocampal levels of KYNA and 3-HAA in the animals treated with 1-DL-MTRP, since the main aim was to prove the involvement of the first step of the KP pathway in CA-induced neurological impairment. It might be envisaged that the inhibition of the KP pathway should also result in a decrease of downstream metabolites, including the neuroprotective KYNA, raising doubts on the role of this metabolite in the beneficial effects of 1-DL-MTRP. It might be considered, however, that many sets of data[91–93] actually show that 1-MT treatment induces a counterintuitive increase of plasmatic KYNA, while producing, as expected, an increase in tryptophan and a decrease in kynurenine and in kynurenine/tryptophan ratio, with no change of 5-HT levels.[92] These data suggest alternative mechanisms of KYNA production, possibly mediated by other tryptophan-degrading enzymes or nonenzymatically.[94] This additional mechanism of action of 1-DL-MTRP, and its involvement for the reduction of CA-induced neurological deficits, requires further investigations.

We recognize some limitations in our study. We investigated the changes in KP activity in the periphery and in the brain by measuring absolute levels of tryptophan, kynurenine, KYNA, and 3-HAA, and we suggest activation of KP based on the ratio between metabolites. However, IDO activation is not the only determinant regulating the peripheral kynurenine/tryptophan ratio.[95] Other factors include: (1) the activity of tryptophan 2,3-dioxygenase (mainly expressed in the liver), which, together with IDO, is responsible for tryptophan→kynurenine conversion in the periphery[32]; and (2) changes in brain influx of permeable KP metabolites (eg, tryptophan and kynurenine). Moreover, changes in downstream enzymatic activity (Figure S1) may underestimate or overestimate the calculated kynurenine/tryptophan ratio, and the influx of kynurenine and tryptophan into the brain may have partially masked the activation of the downstream KP steps. Thus, mRNA expression, protein levels, and the activity of brain and peripheral enzymes of the KP after CA/CPR, need to be investigated to better elucidate which branch of the KP is preferentially activated after CA/CPR.

In conclusion, we uphold the involvement of KP in the neurological deficit following CA/CPR, also demonstrating that the degree of peripheral activation of KP may predict functional outcomes of CA. Further studies are needed to clarify the role of each neuroactive kynurenines in the molecular mechanisms underlying the CA-induced neuropathological events––also considering other downstream metabolites (eg, quinolinic acid)––in order to define KP as a neuroprognostic biomarker after CA/CPR and/or an important pharmacological target to reduce morbidity and mortality after successful CPR.

ARTICLE INFORMATION

Received February 8, 2021; Revised September 3, 2021; accepted September 29, 2021.

Affiliations

Department of Biochemistry and Molecular Pharmacology (J.L., C.F., M.G.); Department of Cardiovascular Medicine (F.F., D.O., R.A., D.D.G., C.P., F.M., L.S., D.N., A.M., R.L.); Department of Environmental Health Sciences (A.P.); and (S.G.), Istituto di Ricerche Farmacologiche Mario Negri IRCCS, Milan, Italy; Department of Anesthesiology, Intensive Care and Emergency, Fondazione IRCCS Ca' Granda Ospedale Maggiore Policlinico, Milan, Italy (G.R.); and Department of Pathophysiology and Transplantation, University of MilanItaly, (G.R.).

Sources of Funding

The study was fully supported by the Associazione Amici del Mario Negri.

Disclosures

None.

Supplementary Material

Data S1
Tables S1–S4
Figures S1–S5
References 96–98

REFERENCES

1. Nolan JP, Neumar RW, Adrie C, Aibiki M, Berg RA, Bottiger BW, Callaway C, Clark RS, Geocadin RG, Jauch EC, et al. Post-cardiac arrest syndrome: epidemiology, pathophysiology, treatment, and prognostication. A scientific statement from the international liaison committee on resuscitation; the american heart association emergency cardiovascular care committee; the council on cardiovascular surgery and anesthesia; the council on cardiopulmonary, perioperative, and critical care; the council on clinical cardiology; the council on stroke. *Resuscitation*. 2008;79:350–379. doi: 10.1016/j.resuscitation.2008.09.017
2. Laver S, Farrow C, Turner D, Nolan J. Mode of death after admission to an intensive care unit following cardiac arrest. *Intensive Care Med*. 2004;30:2126–2128. doi: 10.1007/s00134-004-2425-z
3. Benjamin EJ, Virani SS, Callaway CW, Chamberlain AM, Chang AR, Cheng S, Chiuve SE, Cushman M, Delling FN, Deo R, et al. Heart disease and stroke statistics-2018 update: a report from the American Heart Association. *Circulation*. 2018;137:e67–e492. doi: 10.1161/CIR.0000000000000558
4. Krumholz A, Stern BJ, Weiss HD. Outcome from coma after cardiopulmonary resuscitation: relation to seizures and myoclonus. *Neurology*. 1988;38:401–405. doi: 10.1212/WNL.38.3.401
5. Lilja G, Nielsen N, Bro-Jeppesen J, Dunford H, Friberg H, Hofgren C, Horn J, Insorsi A, Kjaergaard J, Nilsson F, et al. Return to work and participation in society after out-of-hospital cardiac arrest. *Circ Cardiovasc Qual Outcomes*. 2018;11:e003566. doi: 10.1161/CIRCOUTCOMES.117.003566
6. Middelkamp W, Moulaert VR, Verbunt JA, van Heugten CM, Bakx WG, Wade DT. Life after survival: long-term daily life functioning and quality of life of patients with hypoxic brain injury as a result of a cardiac arrest. *Clin Rehabil*. 2007;21:425–431. doi: 10.1177/0269215507075307
7. Moulaert VR, Verbunt JA, van Heugten CM, Wade DT. Cognitive impairments in survivors of out-of-hospital cardiac arrest: a systematic review. *Resuscitation*. 2009;80:297–305. doi: 10.1016/j.resuscitation.2008.10.034
8. Pusswald G, Fertl E, Faltl M, Auff E. Neurological rehabilitation of severely disabled cardiac arrest survivors. Part II. Life situation of patients and families after treatment. *Resuscitation*. 2000;47:241–248. doi: 10.1016/S0300-9572(00)00240-9
9. Sekhon MS, Ainslie PN, Griesdale DE. Clinical pathophysiology of hypoxic ischemic brain injury after cardiac arrest: a "two-hit" model. *Crit Care*. 2017;21:90. doi: 10.1186/s13054-017-1670-9
10. Chalkias A, Xanthos T. Post-cardiac arrest brain injury: pathophysiology and treatment. *J Neurol Sci*. 2012;315:1–8. doi: 10.1016/j.jns.2011.12.007
11. Nolan JP, Soar J, Cariou A, Cronberg T, Moulaert VR, Deakin CD, Bottiger BW, Friberg H, Sunde K, Sandroni C. European Resuscitation Council and European Society of Intensive Care Medicine guidelines for post-resuscitation care 2015: section 5 of the European Resuscitation Council guidelines for resuscitation 2015. *Resuscitation*. 2015;95:202–222. doi: 10.1016/j.resuscitation.2015.07.018
12. Sandroni C, Cariou A, Cavallaro F, Cronberg T, Friberg H, Hoedemaekers C, Horn J, Nolan JP, Rossetti AO, Soar J. Prognostication in comatose survivors of cardiac arrest: an advisory statement from the european resuscitation council and the European Society of Intensive care medicine. *Resuscitation*. 2014;85:1779–1789. doi: 10.1016/j.resuscitation.2014.08.011
13. Sandroni C, D'Arrigo S, Nolan JP. Prognostication after cardiac arrest. *Crit Care*. 2018;22:150. doi: 10.1186/s13054-018-2060-7
14. Ristagno G, Fries M, Brunelli L, Fumagalli F, Bagnati R, Russo I, Staszewsky L, Masson S, Li Volti G, Zappala A, et al. Early kynurenine pathway activation following cardiac arrest in rats, pigs, and humans. *Resuscitation*. 2013;84:1604–1610. doi: 10.1016/j.resuscitation.2013.06.002
15. Shimizu T, Nomiyama S, Hirata F, Hayaishi O. Indoleamine 2,3-dioxygenase. Purification and some properties. *J Biol Chem*. 1978;253:4700–4706. doi: 10.1016/S0021-9258(17)30447-7
16. Yamazaki F, Kuroiwa T, Takikawa O, Kido R. Human indolylamine 2,3-dioxygenase. Its tissue distribution, and characterization of the placental enzyme. *Biochem J*. 1985;230:635–638. doi: 10.1042/bj2300635
17. Campbell BM, Charych E, Lee AW, Moller T. Kynurenines in CNS disease: regulation by inflammatory cytokines. *Front Neurosci*. 2014;8:12. doi: 10.3389/fnins.2014.00012
18. Song P, Ramprasath T, Wang H, Zou MH. Abnormal kynurenine pathway of tryptophan catabolism in cardiovascular diseases. *Cell Mol Life Sci*. 2017;74:2899–2916. doi: 10.1007/s00018-017-2504-2
19. Labadie BW, Bao R, Luke JJ. Reimagining IDO pathway inhibition in cancer immunotherapy via downstream focus on the tryptophan-kynurenine-aryl hydrocarbon axis. *Clin Cancer Res*. 2019;25:1462–1471. doi: 10.1158/1078-0432.CCR-18-2882
20. Rebnord EW, Strand E, Midttun O, Svingen GF, Christensen MH, Ueland PM, Mellgren G, Njolstad PR, Tell GS, Nygard OK, et al. The kynurenine: tryptophan ratio as a predictor of incident type 2 diabetes mellitus in individuals with coronary artery disease. *Diabetologia*. 2017;60:1712–1721. doi: 10.1007/s00125-017-4329-9
21. Eller SK, Däubener W. Role of kynurenine pathway in infections. In: Mittal S, ed. *Targeting the Broadly Pathogenic Kynurenine Pathway*. Springer International Publishing; 2015:179–190.
22. Ogyu K, Kubo K, Noda Y, Iwata Y, Tsugawa S, Omura Y, Wada M, Tarumi R, Plitman E, Moriguchi S, et al. Kynurenine pathway in depression: a systematic review and meta-analysis. *Neurosci Biobehav Rev*. 2018;90:16–25. doi: 10.1016/j.neubiorev.2018.03.023
23. Erhardt S, Schwieler L, Imbeault S, Engberg G. The kynurenine pathway in schizophrenia and bipolar disorder. *Neuropharmacology*. 2017;112:297–306. doi: 10.1016/j.neuropharm.2016.05.020
24. Maddison DC, Giorgini F. The kynurenine pathway and neurodegenerative disease. *Semin Cell Dev Biol*. 2015;40:134–141. doi: 10.1016/j.semcdb.2015.03.002
25. Darcy CJ, Davis JS, Woodberry T, McNeil YR, Stephens DP, Yeo TW, Anstey NM. An observational cohort study of the kynurenine to tryptophan ratio in sepsis: association with impaired immune and microvascular function. *PLoS One*. 2011;6:e21185. doi: 10.1371/journal.pone.0021185
26. Ferrario M, Cambiaghi A, Brunelli L, Giordano S, Caironi P, Guatteri L, Raimondi F, Gattinoni L, Latini R, Masson S, et al. Mortality prediction in patients with severe septic shock: a pilot study using a target metabolomics approach. *Sci Rep*. 2016;6:20391. doi: 10.1038/srep20391
27. Forrest CM, Mackay GM, Oxford L, Millar K, Darlington LG, Higgins MJ, Stone TW. Kynurenine metabolism predicts cognitive function in patients following cardiac bypass and thoracic surgery. *J Neurochem*. 2011;119:136–152. doi: 10.1111/j.1471-4159.2011.07414.x
28. Ristagno G, Latini R, Vaahersalo J, Masson S, Kurola J, Varpula T, Lucchetti J, Fracasso C, Guiso G, Montanelli A, et al. Early activation of the kynurenine pathway predicts early death and long-term outcome in patients resuscitated from out-of-hospital cardiac arrest. *J Am Heart Assoc*. 2014;3:e001094. doi: 10.1161/JAHA.114.001094
29. Adams Wilson JR, Morandi A, Girard TD, Thompson JL, Boomershine CS, Shintani AK, Ely EW, Pandharipande PP. The association of the kynurenine pathway of tryptophan metabolism with acute brain dysfunction during critical illness*. *Crit Care Med*. 2012;40:835–841. doi: 10.1097/CCM.0b013e318236f62d
30. Darlington LG, Mackay GM, Forrest CM, Stoy N, George C, Stone TW. Altered kynurenine metabolism correlates with infarct volume in stroke. *Eur J Neurosci*. 2007;26:2211–2221. doi: 10.1111/j.1460-9568.2007.05838.x
31. Yan EB, Frugier T, Lim CK, Heng B, Sundaram G, Tan M, Rosenfeld JV, Walker DW, Guillemin GJ, Morganti-Kossmann MC. Activation of the kynurenine pathway and increased production of the excitotoxin quinolinic acid following traumatic brain injury in humans. *J Neuroinflammation*. 2015;12:110. doi: 10.1186/s12974-015-0328-2
32. Schwarcz R, Bruno JP, Muchowski PJ, Wu HQ. Kynurenines in the mammalian brain: when physiology meets pathology. *Nat Rev Neurosci*. 2012;13:465–477. doi: 10.1038/nrn3257
33. Chen Y, Guillemin GJ. Kynurenine pathway metabolites in humans: disease and healthy states. *Int J Tryptophan Res*. 2009;2:1–19. doi: 10.4137/IJTR.S2097
34. Stone TW. Neuropharmacology of quinolinic and kynurenic acids. *Pharmacol Rev*. 1993;45:309–379.
35. Stone TW, Addae JI. The pharmacological manipulation of glutamate receptors and neuroprotection. *Eur J Pharmacol*. 2002;447:285–296. doi: 10.1016/S0014-2999(02)01851-4
36. Hilmas C, Pereira EF, Alkondon M, Rassoulpour A, Schwarcz R, Albuquerque EX. The brain metabolite kynurenic acid inhibits alpha7 nicotinic receptor activity and increases non-alpha7 nicotinic receptor expression: physiopathological implications. *J Neurosci*. 2001;21:7463–7473.

37. DiNatale BC, Murray IA, Schroeder JC, Flaveny CA, Lahoti TS, Laurenzana EM, Omiecinski CJ, Perdew GH. Kynurenic acid is a potent endogenous aryl hydrocarbon receptor ligand that synergistically induces interleukin-6 in the presence of inflammatory signaling. *Toxicol Sci*. 2010;115:89–97. doi: 10.1093/toxsci/kfq024
38. Kilkenny C, Browne WJ, Cuthill IC, Emerson M, Altman DG. Improving bioscience research reporting: the arrive guidelines for reporting animal research. *PLoS Biol*. 2010;8:e1000412. doi: 10.1371/journal.pbio.1000412
39. Fumagalli F, Russo I, Staszewsky L, Li Y, Letizia T, Masson S, Novelli D, Rocchetti M, Canovi M, Veglianese P, et al. Ranolazine ameliorates postresuscitation electrical instability and myocardial dysfunction and improves survival with good neurologic recovery in a rat model of cardiac arrest. *Heart Rhythm*. 2014;11:1641–1647. doi: 10.1016/j.hrthm.2014.05.023
40. Adrie C, Laurent I, Monchi M, Cariou A, Dhainaou JF, Spaulding C. Postresuscitation disease after cardiac arrest: a sepsis-like syndrome? *Curr Opin Crit Care*. 2004;10:208–212. doi: 10.1097/01.ccx.0000126090.06275.fe
41. Heyes MP, Saito K, Crowley JS, Davis LE, Demitrack MA, Der M, Dilling LA, Elia J, Kruesi MJ, Lackner A, et al. Quinolinic acid and kynurenine pathway metabolism in inflammatory and non-inflammatory neurological disease. *Brain*. 1992;115:1249–1273. doi: 10.1093/brain/115.5.1249
42. Stoppe C, Fries M, Rossaint R, Grieb G, Coburn M, Simons D, Brucken D, Bernhagen J, Pallua N, Rex S. Blood levels of macrophage migration inhibitory factor after successful resuscitation from cardiac arrest. *PLoS One*. 2012;7:e33512. doi: 10.1371/journal.pone.0033512
43. Wang Y, Liu H, McKenzie G, Witting PK, Stasch JP, Hahn M, Changsirivathanathamrong D, Wu BJ, Ball HJ, Thomas SR, et al. Kynurenine is an endothelium-derived relaxing factor produced during inflammation. *Nat Med*. 2010;16:279–285. doi: 10.1038/nm.2092
44. Kaszaki J, Palasthy Z, Erczes D, Racz A, Torday C, Varga G, Vecsei L, Boros M. Kynurenic acid inhibits intestinal hypermotility and xanthine oxidase activity during experimental colon obstruction in dogs. *Neurogastroenterol Motil*. 2008;20:53–62.
45. Varga G, Erces D, Fazekas B, Fulop M, Kovacs T, Kaszaki J, Fulop F, Vecsei L, Boros M. N-methyl-d-aspartate receptor antagonism decreases motility and inflammatory activation in the early phase of acute experimental colitis in the rat. *Neurogastroenterol Motil*. 2010;22:217–225, e268. doi: 10.1111/j.1365-2982.2009.01390.x
46. Lugo-Huitron R, Blanco-Ayala T, Ugalde-Muniz P, Carrillo-Mora P, Pedraza-Chaverri J, Silva-Adaya D, Maldonado PD, Torres I, Pinzon E, Ortiz-Islas E, et al. On the antioxidant properties of kynurenic acid: free radical scavenging activity and inhibition of oxidative stress. *Neurotoxicol Teratol*. 2011;33:538–547. doi: 10.1016/j.ntt.2011.07.002
47. Brunelli L, Ristagno G, Bagnati R, Fumagalli F, Latini R, Fanelli R, Pastorelli R. A combination of untargeted and targeted metabolomics approaches unveils changes in the kynurenine pathway following cardiopulmonary resuscitation. *Metabolomics*. 2013;9:839–852. doi: 10.1007/s11306-013-0506-0
48. Shoaib M, Choudhary RC, Choi J, Kim N, Hayashida K, Yagi T, Yin T, Nishikimi M, Stevens JF, Becker LB, et al. Plasma metabolomics supports the use of long-duration cardiac arrest rodent model to study human disease by demonstrating similar metabolic alterations. *Sci Rep*. 2020;10:19707. doi: 10.1038/s41598-020-76401-x
49. White BC, Grossman LI, O'Neil BJ, DeGracia DJ, Neumar RW, Rafols JA, Krause GS. Global brain ischemia and reperfusion. *Ann Emerg Med*. 1996;27:588–594. doi: 10.1016/S0196-0644(96)70161-0
50. Wijdicks EF, Campeau NG, Miller GM. Mr imaging in comatose survivors of cardiac resuscitation. *AJNR Am J Neuroradiol*. 2001;22:1561–1565.
51. Cohan CH, Neumann JT, Dave KR, Alekseyenko A, Binkert M, Stransky K, Lin HW, Barnes CA, Wright CB, Perez-Pinzon MA. Effect of cardiac arrest on cognitive impairment and hippocampal plasticity in middle-aged rats. *PLoS One*. 2015;10:e0124918. doi: 10.1371/journal.pone.0124918
52. Putzu A, Valtorta S, Di Grigoli G, Haenggi M, Belloli S, Malgaroli A, Gemma M, Landoni G, Beretta L, Moresco RM. Regional differences in cerebral glucose metabolism after cardiac arrest and resuscitation in rats using [(18)F]FDG positron emission tomography and autoradiography. *Neurocrit Care*. 2018;28:370–378. doi: 10.1007/s12028-017-0445-0
53. Fukui S, Schwarcz R, Rapoport SI, Takada Y, Smith QR. Blood-brain barrier transport of kynurenines: implications for brain synthesis and metabolism. *J Neurochem*. 1991;56:2007–2017. doi: 10.1111/j.1471-4159.1991.tb03460.x
54. Park JS, You Y, Min JH, Yoo I, Jeong W, Cho Y, Ryu S, Lee J, Kim SW, Cho SU, et al. Study on the timing of severe blood-brain barrier disruption using cerebrospinal fluid-serum albumin quotient in post cardiac arrest patients treated with targeted temperature management. *Resuscitation*. 2019;135:118–123. doi: 10.1016/j.resuscitation.2018.10.026
55. Pluta R, Lossinsky AS, Wisniewski HM, Mossakowski MJ. Early blood-brain barrier changes in the rat following transient complete cerebral ischemia induced by cardiac arrest. *Brain Res*. 1994;633:41–52. doi: 10.1016/0006-8993(94)91520-2
56. Sharma HS, Miclescu A, Wiklund L. Cardiac arrest-induced regional blood-brain barrier breakdown, edema formation and brain pathology: a light and electron microscopic study on a new model for neurodegeneration and neuroprotection in porcine brain. *J Neural Transm (Vienna)*. 2011;118:87–114. doi: 10.1007/s00702-010-0486-4
57. Owe-Young R, Webster NL, Mukhtar M, Pomerantz RJ, Smythe G, Walker D, Armati PJ, Crowe SM, Brew BJ. Kynurenine pathway metabolism in human blood-brain-barrier cells: implications for immune tolerance and neurotoxicity. *J Neurochem*. 2008;105:1346–1357. doi: 10.1111/j.1471-4159.2008.05241.x
58. Guillemin GJ, Smith DG, Smythe GA, Armati PJ, Brew BJ. Expression of the kynurenine pathway enzymes in human microglia and macrophages. *Adv Exp Med Biol*. 2003;527:105–112. doi: 10.1007/978-1-4615-0135-0_12
59. Rodgers J, Stone TW, Barrett MP, Bradley B, Kennedy PG. Kynurenine pathway inhibition reduces central nervous system inflammation in a model of human African trypanosomiasis. *Brain*. 2009;132:1259–1267. doi: 10.1093/brain/awp074
60. Gal EM, Sherman AD. Synthesis and metabolism of l-kynurenine in rat brain. *J Neurochem*. 1978;30:607–613. doi: 10.1111/j.1471-4159.1978.tb07815.x
61. Speciale C, Hares K, Schwarcz R, Brookes N. High-affinity uptake of L-kynurenine by a Na+-independent transporter of neutral amino acids in astrocytes. *J Neurosci*. 1989;9:2066–2072. doi: 10.1523/JNEUROSCI.09-06-02066.1989
62. Alberati-Giani D, Ricciardi-Castagnoli P, Kohler C, Cesura AM. Regulation of the kynurenine pathway by IFN-gamma in murine cloned macrophages and microglial cells. *Adv Exp Med Biol*. 1996;398:171–175. doi: 10.1007/978-1-4613-0381-7_28
63. Braidy N, Guillemin GJ, Grant R. Effects of kynurenine pathway inhibition on NAD metabolism and cell viability in human primary astrocytes and neurons. *Int J Tryptophan Res*. 2011;4:29–37. doi: 10.4137/IJTR.S7052
64. Guidetti P, Hoffman GE, Melendez-Ferro M, Albuquerque EX, Schwarcz R. Astrocytic localization of kynurenine aminotransferase II in the rat brain visualized by immunocytochemistry. *Glia*. 2007;55:78–92. doi: 10.1002/glia.20432
65. Guillemin GJ, Kerr SJ, Smythe GA, Smith DG, Kapoor V, Armati PJ, Croitoru J, Brew BJ. Kynurenine pathway metabolism in human astrocytes: a paradox for neuronal protection. *J Neurochem*. 2001;78:842–853. doi: 10.1046/j.1471-4159.2001.00498.x
66. Guillemin GJ, Smith DG, Kerr SJ, Smythe GA, Kapoor V, Armati PJ, Brew BJ. Characterisation of kynurenine pathway metabolism in human astrocytes and implications in neuropathogenesis. *Redox Rep*. 2000;5:108–111. doi: 10.1179/135100000101535375
67. Heyes MP, Achim CL, Wiley CA, Major EO, Saito K, Markey SP. Human microglia convert l-tryptophan into the neurotoxin quinolinic acid. *Biochem J*. 1996;320:595–597. doi: 10.1042/bj3200595
68. Denes A, Vidyasagar R, Feng J, Narvainen J, McColl BW, Kauppinen RA, Allan SM. Proliferating resident microglia after focal cerebral ischaemia in mice. *J Cereb Blood Flow Metab*. 2007;27:1941–1953. doi: 10.1038/sj.jcbfm.9600495
69. Ouyang YB, Voloboueva LA, Xu LJ, Giffard RG. Selective dysfunction of hippocampal CA1 astrocytes contributes to delayed neuronal damage after transient forebrain ischemia. *J Neurosci*. 2007;27:4253–4260. doi: 10.1523/JNEUROSCI.0211-07.2007
70. Sulkowski G, Bubko I, Struzynska L, Januszewski S, Walski M, Rafalowska U. Astrocytic response in the rodent model of global cerebral ischemia and during reperfusion. *Exp Toxicol Pathol*. 2002;54:31–38. doi: 10.1078/0940-2993-00229
71. Suma T, Koshinaga M, Fukushima M, Kano T, Katayama Y. Effects of in situ administration of excitatory amino acid antagonists on rapid

microglial and astroglial reactions in rat hippocampus following traumatic brain injury. *Neurol Res*. 2008;30:420–429. doi: 10.1179/016164107X251745
72. Xiang Y, Zhao H, Wang J, Zhang L, Liu A, Chen Y. Inflammatory mechanisms involved in brain injury following cardiac arrest and cardiopulmonary resuscitation. *Biomed Rep*. 2016;5:11–17. doi: 10.3892/br.2016.677
73. Amori L, Guidetti P, Pellicciari R, Kajii Y, Schwarcz R. On the relationship between the two branches of the kynurenine pathway in the rat brain in vivo. *J Neurochem*. 2009;109:316–325. doi: 10.1111/j.1471-4159.2009.05893.x
74. Guillemin GJ, Smythe G, Takikawa O, Brew BJ. Expression of indoleamine 2,3-dioxygenase and production of quinolinic acid by human microglia, astrocytes, and neurons. *Glia*. 2005;49:15–23. doi: 10.1002/glia.20090
75. Heyes MP, Chen CY, Major EO, Saito K. Different kynurenine pathway enzymes limit quinolinic acid formation by various human cell types. *Biochem J*. 1997;326:351–356. doi: 10.1042/bj3260351
76. Schwarcz R, Stone TW. The kynurenine pathway and the brain: challenges, controversies and promises. *Neuropharmacology*. 2017;112:237–247. doi: 10.1016/j.neuropharm.2016.08.003
77. Gonzalez Esquivel D, Ramirez-Ortega D, Pineda B, Castro N, Rios C. Pérez de la Cruz V. Kynurenine pathway metabolites and enzymes involved in redox reactions. *Neuropharmacology*. 2017;112:331–345. doi: 10.1016/j.neuropharm.2016.03.013
78. Pierozan P, Zamoner A, Soska AK, Silvestrin RB, Loureiro SO, Heimfarth L, Mello e Souza T, Wajner M, Pessoa-Pureur R. Acute intrastriatal administration of quinolinic acid provokes hyperphosphorylation of cytoskeletal intermediate filament proteins in astrocytes and neurons of rats. *Exp Neurol*. 2010;224:188–196. doi: 10.1016/j.expneurol.2010.03.009
79. Rahman A, Ting K, Cullen KM, Braidy N, Brew BJ, Guillemin GJ. The excitotoxin quinolinic acid induces tau phosphorylation in human neurons. *PLoS One*. 2009;4:e6344. doi: 10.1371/journal.pone.0006344
80. Hou DY, Muller AJ, Sharma MD, DuHadaway J, Banerjee T, Johnson M, Mellor AL, Prendergast GC, Munn DH. Inhibition of indoleamine 2,3-dioxygenase in dendritic cells by stereoisomers of 1-methyl-tryptophan correlates with antitumor responses. *Cancer Res*. 2007;67:792–801. doi: 10.1158/0008-5472.CAN-06-2925
81. Peterson AC, Migawa MT, Martin MJ, Hamaker LK, Czerwinski KM, Zhang W, Arend RA, Fisette PL, Ozaki Y, Will JA. Evaluation of functionalized tryptophan derivatives and related compounds as competitive inhibitors of indoleamine 2, 3-dioxygenase. *Med Chem Res*. 1994;3:531–544.
82. Prendergast GC, Malachowski WP, DuHadaway JB, Muller AJ. Discovery of IDO1 inhibitors: from bench to bedside. *Cancer Res*. 2017;77:6795–6811. doi: 10.1158/0008-5472.CAN-17-2285
83. Jia L, Schweikart K, Tomaszewski J, Page JG, Noker PE, Buhrow SA, Reid JM, Ames MM, Munn DH. Toxicology and pharmacokinetics of 1-methyl-d-tryptophan: absence of toxicity due to saturating absorption. *Food Chem Toxicol*. 2008;46:203–211. doi: 10.1016/j.fct.2007.07.017
84. Wirthgen E, Kanitz E, Tuchscherer M, Tuchscherer A, Domanska G, Weitschies W, Seidlitz A, Scheuch E, Otten W. Pharmacokinetics of 1-methyl-l-tryptophan after single and repeated subcutaneous application in a porcine model. *Exp Anim*. 2016;65:147–155. doi: 10.1538/expanim.15-0096
85. Hayashida K, Sano M, Kamimura N, Yokota T, Suzuki M, Maekawa Y, Kawamura A, Abe T, Ohta S, Fukuda K, et al. H(2) gas improves functional outcome after cardiac arrest to an extent comparable to therapeutic hypothermia in a rat model. *J Am Heart Assoc*. 2012;1:e003459. doi: 10.1161/JAHA.112.003459
86. Colpo GD, Venna VR, McCullough LD, Teixeira AL. Systematic review on the involvement of the kynurenine pathway in stroke: preclinical and clinical evidence. *Front Neurol*. 2019;10:778. doi: 10.3389/fneur.2019.00778
87. Gong J, Ju YN, Wang XT, Zhu JL, Jin ZH, Ga W. Corrigendum to "Ac2-26 ameliorates lung ischemia-reperfusion injury via the enos pathway" [biomed. Pharmacother. 117 (2019) 109194]. *Biomed Pharmacother*. 2020;130:110760. doi: 10.1016/j.biopha.2020.110760
88. Gong J, Tai QH, Xu GX, Wang XT, Zhu JL, Zhao XQ, Sun HB, Zhu D, Gao W. Ac2-26 alleviates brain injury after cardiac arrest and cardiopulmonary resuscitation in rats via the eNOS pathway. *Mediators Inflamm*. 2020;2020:3649613. doi: 10.1155/2020/3649613
89. Liu J, Nolte K, Brook G, Liebenstund L, Weinandy A, Hollig A, Veldeman M, Willuweit A, Langen KJ, Rossaint R, et al. Post-stroke treatment with argon attenuated brain injury, reduced brain inflammation and enhanced m2 microglia/macrophage polarization: a randomized controlled animal study. *Crit Care*. 2019;23:198. doi: 10.1186/s13054-019-2493-7
90. Brouns R, Verkerk R, Aerts T, De Surgeloose D, Wauters A, Scharpe S. De Deyn PP. The role of tryptophan catabolism along the kynurenine pathway in acute ischemic stroke. *Neurochem Res*. 2010;35:1315–1322. doi: 10.1007/s11064-010-0187-2
91. Kiank C, Zeden JP, Drude S, Domanska G, Fusch G, Otten W, Schuett C. Psychological stress-induced, IDO1-dependent tryptophan catabolism: implications on immunosuppression in mice and humans. *PLoS One*. 2010;5:e11825. doi: 10.1371/journal.pone.0011825
92. Wirthgen E, Leonard AK, Scharf C, Domanska G. The immunomodulator 1-methyltryptophan drives tryptophan catabolism toward the kynurenic acid branch. *Front Immunol*. 2020;11:313. doi: 10.3389/fimmu.2020.00313
93. Wirthgen E, Otten W, Tuchscherer M, Tuchscherer A, Domanska G, Brenmoehl J, Gunther J, Ohde D, Weitschies W, Seidlitz A, et al. Effects of 1-methyltryptophan on immune responses and the kynurenine pathway after lipopolysaccharide challenge in pigs. *Int J Mol Sci*. 2018;19. doi: 10.3390/ijms19103009
94. Ramos-Chavez LA, Lugo Huitron R, Gonzalez Esquivel D, Pineda B, Rios C, Silva-Adaya D, Sanchez-Chapul L, Roldan-Roldan G, Pérez de la Cruz V. Relevance of alternative routes of kynurenic acid production in the brain. *Oxid Med Cell Longev*. 2018;2018:1–14. doi: 10.1155/2018/5272741
95. Badawy AA, Guillemin G. The plasma [kynurenine]/[tryptophan] ratio and indoleamine 2,3-dioxygenase: time for appraisal. *Int J Tryptophan Res*. 2019;12:1178646919868978. doi: 10.1177/1178646919868978
96. Iv P, Weil MH, Mv P, Bisera J, Bruno S, Gazmuri RJ, Rackow EC. Cardiopulmonary resuscitation in the rat. *J Appl Physiol*. 1988;65:2641–2647. doi: 10.1152/jappl.1988.65.6.2641
97. Lang RM, Badano LP, Mor-Avi V, Afilalo J, Armstrong A, Ernande L, Flachskampf FA, Foster E, Goldstein SA, Kuznetsova T, et al. Recommendations for cardiac chamber quantification by echocardiography in adults: an update from the American Society of Echocardiography and the European Association of Cardiovascular Imaging. *J Am Soc Echocardiogr*. 2015;28:1–39.e14. doi: 10.1016/j.echo.2014.10.003
98. Nagueh SF, Smiseth OA, Appleton CP, Byrd BF III, Dokainish H, Edvardsen T, Flachskampf FA, Gillebert TC, Klein AL, Lancellotti P, et al. Recommendations for the evaluation of left ventricular diastolic function by echocardiography: an update from the American Society of Echocardiography and the European Association of Cardiovascular Imaging. *J Am Soc Echocardiogr*. 2016;29:277–314. doi: 10.1016/j.echo.2016.01.011

SUPPLEMENTAL MATERIAL

Data S1.

SUPPLEMENTAL METHODS

(1) Animal preparation

Sprague-Dawley rats were used. Rats were acclimatized to housing, food and water conditions for four days before the experiments. Housing was always specific pathogen free and the rats were co-housed in polycarbonate solid-bottom cages in a temperature-controlled environment (22 ± 2°), with 45-65% humidity and 12h light-dark cycle, with free access to #2018S ENVIGO Rodent Diet (Sterilizable, Pellet) and reverse-osmosis-filtered water. Before surgery, animals were fasted overnight, with free access to water. They were anesthetized by intraperitoneal (IP) injection of thiopental (50 mg/kg). Additional doses of thiopental (10 mg/kg) were given at intervals of approximately 40 minutes or when required to maintain anaesthesia. Ampicillin (50 mg/kg) was injected intramuscularly (IM) as prophylaxis after induction of anaesthesia. Animals were then instrumented for hemodynamic measurements and induction of cardiac arrest (CA), according to an established model of electrically induced CA and cardiopulmonary resuscitation (CPR) [39] as detailed below. Briefly, the trachea was orally intubated with a 14-gauge cannula. A PE-50 catheter was advanced into the descending aorta from the left femoral artery for measurements of arterial pressure (systolic, median and diastolic arterial pressure: SAP, MAP and DAP, see M*easurements methods*) and blood sampling. Through the left external jugular vein, another PE-50 catheter was advanced into the right atrium for measurement of right atrial pressure (RAP) and for the administration of epinephrine. Aortic and right atrial pressures were measured with reference to the mid-chest with conventional external pressure transducers. A 3-Fr PE catheter was advanced through the right external jugular vein into the right atrium. A pre-curved guide wire supplied with

the catheter was then advanced through the catheter into the right ventricle for inducing CA. All catheters were flushed intermittently with saline containing 2.5 IU/mL of bovine heparin. A conventional lead II electrocardiogram (ECG) was continuously monitored. Temperature was monitored with the aid of a rectal probe and maintained at 37±0.5 ºC.

(2) Cardiac arrest (CA) and cardiopulmonary resuscitation (CPR) procedures

Ventricular fibrillation (VF) was electrically induced with progressive increases in 60-Hz current to a maximum of 4 mA delivered to the right ventricular endocardium. The current flow was maintained for 3 min to prevent spontaneous defibrillation. Animals were subjected to 7 minutes (aim #1) or 8 minutes (aim #2) of untreated VF following by precordial compression (PC) with a pneumatically driven mechanical chest compressor as previously described [96]. The PC depth was adjusted to ensure *coronary perfusion pressure* (CPP) at least of 25 mmHg. The PC rate was 200/min with equal compression-decompression. From the start of PC, animals were mechanically ventilated at a frequency of 50/min with tidal volume 0.6 mL/100g and FiO_2 1.0. A single dose of epinephrine (0.02 mg/kg) was injected into the right atrium 2 min after the start of PC. After 5 minutes (aim #1) or 8 minutes (aim #2) of CPR, resuscitation was attempted with up to three 2-joule (J) defibrillations (CodeMaster XL, Philips Heartstream). ROSC was defined as the return of supraventricular rhythm with MAP > 50 mmHg for at least 5 minutes. If ROSC did not occur, two more 30-seconds cycles CPR were done with counter-shock. After ROSC, mechanical ventilation was maintained at FiO_2 1 for 1h post-resuscitation, then continued with FiO_2 0.21.

(3) Measurements

Aortic and right atrial pressures, and electrocardiogram (AP, RAP and ECG) were continuously recorded with a personal computer-based data acquisition system supported by CODAS hard

hardware and software (DataQ, Akron, OH). Coronary perfusion pressure (CPP) was calculated as the difference between aortic and time-coincident right atrial pressures. Time to ROSC is calculated as the time from start of CPR to return of spontaneous circulation, and includes additional chest compression cycles and subsequent defibrillations.

Myocardial function was assessed by transthoracic echocardiography 4 and 96 hours post-ROSC using an SSD-5500 (Aloka, Mitaka, Tokyo, Japan) equipped with a 13 MHz linear array transducer at high frame-rate imaging (102 Hz) and a 7,5 MHz phase array probe for pulse wave, colour and tissue Doppler imaging. Rats undergoing echocardiography at 96 hours were anesthetized with thiopental IP 50 mg/kg (and if necessary 10 mg/kg recall doses). The aim of this test was to examine left ventricular (LV) structure and systolic and diastolic function after cardiac arrest. Mono- and bi-dimensional (2D) echocardiography were followed and images from parasternal long- and short-axis, apical four and five chamber views were acquired. Using Pulsed Wave Doppler echocardiography was used to record transmitral and transaortic flow. Tissue Doppler Imaging (TDI) of LV lateral and septal mitral anulus were evaluated. The assessed parameters were: heart rate (HR), LV outflow tract diameter (LVOT), end-systolic and end-diastolic LV wall thicknesses, end-diastolic and end-systolic diameters, shortening fraction (SF), E/e' ratio, LV end-systolic and end-diastolic volumes (ESV μL; EDV μL), ejection fraction (EF) and LV cardiac output (CO). All recordings and measurements were followed according to the recommendations of the American and European Societies of Echocardiography Guidelines [97, 98].

Left ventricular EF (LVEF, %) is an indicator of systolic function, calculated as (LVEDV-LVESV) / (LVEDV)*100. End-diastole is preferably defined as the first frame after mitral valve closure or the frame in the cardiac cycle in which the respective LV dimension is the largest. End-systole is best defined as the frame after aortic valve closure or the frame in which the cardiac dimension or volume is smallest. Volumetric measurements are usually based on tracings of the interface between the compacted myocardium and the LV cavity. LV areas were measured and LV volumes were calculated by modified Simpson's single plane rule from the parasternal long-axis view.

The pulse Doppler peak mitral inflow velocity (peak E wave) (μm/sec) to tissue Doppler e' wave velocity ratio (μm/sec) (E/e') is an indicator of diastolic function. TDI was obtained from the apical four-chamber view placing a 1.0-mm sample at the septal and lateral junction of the mitral annulus. The normal E/e′ ratio should be ≤9.

Flow across a fixed orifice is the product of the cross-sectional area (CSA) of the orifice and flow velocity. Because flow velocity varies during ejection in a pulsatile system such as the cardiovascular system, individual velocities of the Doppler spectrum need to be summed or integrated to measure the total flow volume during a given ejection period. The sum of velocities is called the Time Velocity Integral (TVI; μm/sec). Once TVI has been determined, SV (μL) is calculated by multiplying TVI by CSA. The location most frequently used to determine SV is the left ventricle outflow tract (LVOT). Cardiac output (CO, μL/min) represents the blood flow passing through the LVOT per unit of time. CO was calculated using the formula: CO = SV*HR. CO was obtained from the apical five-chamber view placing a 1.0-mm sample volume at the aortic valve. To evaluate the recovery in CO for each group, data were analysed as relative changes (%) for each single animal as delta CO (%) = $[(CO_{96h} - CO_{4h})/CO_{4h}]*100$. For the 1-DL-MTRP- and Vehicle-treated groups, we calculated the averages.

(4) HPLC-MS/MS methods

Chemicals and reagents. Acetonitrile (ACN), methanol (MeOH), acetic acid (CH_3COOH) and formic acid (HCOOH) were from Sigma-Aldrich Co. (Milan, Italy); all solvents were of liquid chromatography-mass spectrometry (LC-MS) grade. LC-MS grade water was obtained in-house with a Milli-Q system (Millipore, Bedford, MA, USA). L-Tryptophan (TRP), L-kynurenine (KYN), kynurenic acid (KYNA) 3-hydroxyanthranilic acid (3-HAA), serotonin (5-HT) and 1-methyl-DL-tryptophan (1-DL-MTRP) were from Sigma-Aldrich. TRP-d5 and KYNA-d5 were from CDN Isotopes (Chemical Research 2000, Rome, Italy); KYN-d4, and 3-HAA-d2 were from Buchem BV (Apeldoorn, The Netherlands).

Stock and working solutions for plasma analysis. Stock solutions of TRP and KYN reference standard were prepared in CH_3COOH 0.08 M at 1 mg/mL, and diluted together in the same solvent to give a standard working solution containing TRP and KYN at 250 µg/mL and 10 µg/mL respectively. This standard working solution was then serially diluted to give six other standard working solutions at 200, 150, 100, 50, 25 and 6.25 µg TRP/mL and 8.0, 6.0 4.0, 2.0, 1.0 and 0.25 µg KYN/mL.

A stock solution containing KYNA and 3-HAA reference standards at 1 mg/mL were prepared in H_2O and diluted in the same aqueous solvent to give a single standard working solution of 150 ng/mL. Stock solution of 1-DL-MTRP reference standard was prepared in CH_3COOH 0.08M at 1 mg/mL, and diluted in the same solvent to give seven standard working solutions containing 300, 250, 200, 100, 50, 10 and 2.5 µg/mL. Three quality control (QC) working solutions containing both TRP and KYN in CH_3COOH 0.08M at i) 187.5, 125 and 18.75 µg TRP/mL and ii) 7.5, 5.0 and 0.75 µg KYN/mL were used to prepare QC samples. Three QC working solutions containing 1-DL-MTRP in CH_3COOH 0.08M at 225, 150 and 75 µg/mL were used to prepare QC samples (only for aim #2). A single QC working solution containing both KYNA and 3-HAA in H_2O at 150 ng/mL were used to prepare QC samples. Stock and working solutions were stored at -20°C until use.

Stock and working solutions for analysis in hippocampus. Stock solutions of TRP, KYN and 5-HT reference standard were prepared in CH_3COOH 0.08M at 1 mg/mL, and diluted together in the same solvent to give a standard working solution containing TRP at 150 µg/mL, and KYN and 5-HT at 9 µg/mL. This working solution was then serially diluted to give six other standard working solutions at 125, 100, 75, 37.5, 12.5 and 2.5 µg TRP/mL and 7.5, 6.0, 4.5, 2.25 0.75 and 0.15 µg KYN/mL. A stock solution of 1-DL-MTRP reference standard was prepared in CH_3COOH 0.08M at 1 mg/mL and diluted in the same solvent to give seven standard working solutions containing 300, 250, 200, 100, 50, 10 and 2.5 µg/mL. A stock solution containing both KYNA and 3-HAA reference standards at 1 mg/mL were prepared in H_2O and diluted in the same aqueous solvent to give the single standard working solution of 50 ng/mL. Three quality control (QC) working solutions containing both TRP, KYN and 5-HT in CH_3COOH 0.08M at i) 125.0, 75 and 7.5 µg TRP/mL, ii) 7.5, 5.0 and 0.75 µg KYN/mL or 5-HT/mL were used to prepare QC samples. Three QC working solutions containing 1-DL-MTRP in CH_3COOH 0.08M at 225, 150 and 75 µg/mL were used to prepare QC samples (only for aim #2). The same QC working solution for KYNA and 3-HAA prepared for plasma analysis were used for hippocampus. Stock and working solutions were stored at -20°C until use.

Stock and working solutions of internal standards. For both plasma and hippocampal analysis, the same stock solutions and working solutions of internal standards were used. Stock solutions of TRP-d5 and KYN-d4 were prepared in CH_3COOH 0.08M at 1 mg/mL (sol. A) and 100 µg/mL (sol. B) respectively, and a stock solution containing both KYNA-d5 and 3-HAA-d2 was prepared in H_2O at 1 mg/mL, then diluted to 10 µg/mL in CH_3COOH 0.08M (sol. C). Appropriate volumes of 'sol. A', 'sol. B' and 'sol. C' (the latter only for *aim #1*) were combined and diluted with CH_3COOH 0.08M to obtain the final IS working solution containing 100 µg TRP-d5/mL, 5 µg KYN-d4/mL, 0.24 µg KYNA-d5/mL and 0.24 µg 3-HAA-d2/mL.

Plasma samples preparation. Seven-point calibration curves were generated by spiking 100 µL of control plasma with i) 10 µL of the seven TRP/KYN working solutions (for *aim #1* and *#2*), ii) different volumes (0.8 – 32 µL) of the single KYNA/3-HAA working solution (150 ng/mL) (only for *aim #1*) and iii) 10 µL of the seven 1-DL-MTRP working solutions (only for *aim #2*), to have final concentrations in the ranges 0.5-20 µg TRP/mL, 0.025-1 µg KYN/mL, 1.2-48 ng KYNA/mL, 1.2-48 ng 3-HAA/mL and 0.25-30 µg 1-DL-MTRP/mL.

QC samples were prepared by spiking 100 µL of control plasma with i) 10 µL of TRP/KYN QC working solutions (for *aims #1* and *#2*), ii) different volumes of KYNA/3-HAA QC working solution (only for *aim #1*) and iii) 10 µL of 1-DL-MTRP QC working solutions (only for *aim #2*) to final concentrations of 18.75 µg TRP/mL, 0.75 µg KYN/mL, 4 ng KYNA/mL, 4 ng 3-HAA/mL and 22.50 µg 1-DL-MTRP/mL (high quality controls, HQCs), 12.50 µg TRP/mL, 0.50 µg KYN/mL, 18 ng KYNA/mL, 18 ng 3-HAA/mL and 15.0 µg 1-DL-MTRP/mL (mid-quality controls, MQCs), and 0.1875 µg TRP/mL, 0.075 µg KYN/mL, 36 ng KYNA/mL, 36 ng 3-HAA/mL and 0.75 µg 1-DL-MTRP/mL (low-quality controls, LQCs).

Since we added different volumes of the KYNA/3-HAA working and QC solutions in each standard sample (maximum volume added 32 µL), appropriate volumes of H_2O were added to give the same total volume in each sample. Thus, to unknown samples we added 10 µL (*aim #1*) or 20 µL (*aim #2*) of CH_3COOH 0.08M, and 32 µL of H_2O (*aim #1*) before extraction.

Hippocampus samples preparation. Six-point calibration curves were generated by spiking 500 µL of control hippocampal homogenate (1g in 5 mL of H_2O/ACN, 1:2, v/v) with i) 10 µL of the seven TRP/KYN working solutions (for *aims #1* and *#2*), ii) different volumes (0.5-24 µL) of the single KYNA/3-HAA working solution (50 ng/mL) (only for the *aim #1*) and iii) 2 µL of 1-Dl-MTRP working solutions (only *aim #2*), to final concentrations in the ranges 0.25-15 µg TRP/g, 0.015-0.9 µg KYN/g, 0.015-0.9 µg 5-HT/g, 0.25-12 ng KYNA/g, 0.25-12 ng 3-HAA/g and 0.05-6 µg 1-DL-MTRP/g.

QC samples were prepared by spiking 100 µL of control plasma with i) 10 µL of TRP/KYN QC working solutions (for *aims #1* and *#2*), ii) different volumes of KYNA/3-HAA QC working solution (only for *aim #1*) and iii) 2 µL of 1-DL-MTRP QC working solutions (only for *aim #2*) to give final concentrations of 12.50 µg TRP/g, 0.75 µg KYN/g, 10 ng KYNA/g, 10 ng 3-HAA/g, 0.75 µg 5-HT/mL and 4.5 µg 1-DL-MTRP/g, (high quality controls, HQCs), 7.5 µg TRP/g, 0.50 µg KYN/g, 4.0 ng KYNA/g, 4.0 ng 3-HAA/g, 0.45 µg 5-HT/mL and 3.0 µg 1-DL-MTRP/g (mid-quality controls, MQCs), and 0.75 µg TRP/g, 0.075 µg KYN/g, 0.75 ng KYNA/g, 0.75 ng 3-HAA/g, 0.045 µg 5-HT/g and 0.15 µg 1-DL-MTRP/g (low-quality controls, LQCs).

Since we added different volume of the KYNA/3-HAA working and QC solutions in each standard sample (maximum volume added 24 µL), appropriate volumes of H_2O were added to give the same total volume in each sample. Thus, to unknown samples we added 10 µL (*aim #1*) or 12 µL (*aim #2*) of CH_3COOH 0.08M, and 24 µL of H_2O (*aim #1*) before extraction.

Extraction from plasma and hippocampus. Ten µL of deuterated internal standards solution were added to 100 µL of plasma or 500 µL (for standard curves and QCs) of hippocampal homogenate. For unknown samples, resulting homogenate volumes were <500 µL since hippocampus weighted around 30 mg (homogenization ratio: 1g in 5 mL of H_2O/ACN, 1:2, v/v); thus, all volumes were analyzed and a weight correction factor was apply to determine the actual concentration of metabolites. Plasma samples were then mixed with 400 µL of cold CH_3OH, incubated for a 1h at -20°C to allow protein precipitation and then centrifuged at 14000 g for 10 min at 4°C. Hippocampal homogenates were directly centrifuged as plasma. After centrifugation, supernatants were dried under N_2 and the residue was re-suspended in 100 µL of 0.1% HCOOH in water/ACN (99/1, v/v), and injected into the HPLC system coupled to the mass spectrometer.

Aim #1 - Quantitative HPLC-ESI-TripleQ method. The optimized mass spectrometric parameters for gas temperature, gas flow, nebulizer and capillary were respectively 350°C, 10 L/min, 30 psi and 3000 V. Chromatographic separation was done on an Agilent 1200 system

(Agilent Technologies) using an Atlantis T3 column (150 × 2.1 mm; 3 μm particle size, Waters), with an Atlantis T3 VanGuard Cartridge (2.1 mm x 5 mm; 3 μm particle size, Waters). The elution solvents were 0.1% HCOOH in water (mobile phase A, MP-A) and acetonitrile (mobile phase B, MP-B). The injection volume was 20 μL and the flow rate 160 μL/min. The auto-sampler temperature was maintained at 6°C. Elution started with 99% of MP-A and 1% MP-B for 1 min, followed by a 12-min linear gradient to 60% of MP-B, a 2-min linear gradient to 99% of MP-B which was maintained for 2 min, and a 1-min linear gradient to 99% MP-A which was maintained for 8 min to equilibrate the column. The total run time was 26 min. Retention times were 8.8 min (KYN), 8.7 min (KYN-d4), 12.4 min (3-HAA), 12.3 min (3-HAA-d2), 10.1 min (TRP), 10.0 min (TRP-d5), 10.8 min (KYNA) and 10.7 min (KYNA-d5). Mass spectrometric analyses were done using multiple reaction monitoring (MRM) mode, measuring the fragmentation product of the protonated molecular ions of TRP, KYN, KYNA, 3-HAA and the IS. The mass spectrometer Triple Quad 6410 (Agilent Technologies, CA, USA) was equipped with an electrospray ionization source (ESI) operating in positive ion mode. The mass transitions for MRM acquisition and quantification of KP metabolites are shown below:

- TRP: *m*/*z* 205 → *m*/*z* 146, collision energy 14 V
- KYN: *m*/*z* 209 → *m*/*z* 146, collision energy 20 V
- KYNA: *m*/*z* 190 → *m*/*z* 144, collision energy 16 V
- 3-HAA: *m*/*z* 154 → *m*/*z* 80, collision energy 30 V
- TRP-d5: *m*/*z* 210 → *m*/*z* 150, collision energy 16 V
- KYN-d4: *m*/*z* 213 → *m*/*z* 150, collision energy 20 V
- KYNA-d5: *m*/*z* 195 → *m*/*z* 149, collision energy 16 V
- 3-HAA-d2: *m*/*z* 156 → *m*/*z* 82, collision energy 30 V

The HPLC-MS/MS system was controlled by MassHunter (Agilent Technologies) and data were collected and elaborated with the same software.

Aim #2 - Quantitative HPLC-ESI-TripleQ method. Chromatographic separation was done on an Alliance 2695 (Waters Corp.) using an Accucore PFP column (150 × 2.1 mm; 2.6 μm particle size, Thermo-Scientific) at 30°C, with an Accucore PFP guard column defender (10 x 2.1 mm; 2.6 μm particle size, Thermo-Scientific). The elution solvents were 0.1% HCOOH in water (mobile phase A, MP-A) and acetonitrile (mobile phase B, MP-B). The injection volume was 40 μL and the flow rate 200 μL/min. The auto-sampler temperature was maintained at 6°C.

Elution started with 99% of MP-A and 1% MP-B for 2 min, followed by an 18-min linear gradient to 50% of MP-B, a 1-min linear gradient to 70% of MP-B maintained for 1 min, and a 1-min linear gradient to 99% of MP-A which was maintained for 12 min to equilibrate the column. The total run time was 35 min. Retention times were 6.4 min (KYN), 6.3 min (KYN-d4), 12.4 min (TRP), 12.3 min (TRP-d5) and 15.4 min (1-DL-MTRP). Mass spectrometric analyses were done using multiple reaction monitoring (MRM) mode, measuring the fragmentation product of the protonated pseudo-molecular ions of TRP, KYN 1-DL-MTRP and the IS. The mass spectrometer Quattro Micro API triple quadrupole instrument (Waters Corp., Manchester, UK) was equipped with an electrospray ionization source (ESI) operating in positive ion mode. The mass transitions for MRM acquisition and quantification of KP metabolites are shown below:

- TRP: *m*/*z* 205.2 → *m*/*z* 188.2; cone 15 V, collision energy 5 eV
- KYN: *m*/*z* 209.5 → *m*/*z* 192.1; cone 15 V, collision energy 5 eV
- 5-HT: *m*/*z* 177.0 → *m*/*z* 160.2; cone 15 V, collision energy 10 eV
- 1-DL-MTRP: *m*/*z* 219.1 → *m*/*z* 160.1; cone 15 V, collision energy 15 eV
- TRP-d5: *m*/*z* 445.1 → *m*/*z* 428.1; cone 20 V, collision energy 8 eV
- KYN-d4: *m*/*z* 445.1 → *m*/*z* 428.1; cone 15 V, collision energy 10 eV

The optimized mass spectrometric parameters for capillary, extractor and RF lens voltages were respectively 3.5 kV, 1.0 V and 2.0 V. The source and desolvation temperatures were 100 and 300°C. The desolvation and cone gas flows were 600 and 60 L/h. Argon was used as collision gas.

The HPLC-MS/MS system was controlled by the MassLynx® version 4.1 (Waters Corp.) and data were collected with the same software.

(5) Real-Time Polymerase Chain Reaction (RT-PCR) (*aim* #2)

Total RNA was extracted from the brain cortex of rats pre-treated with vehicle or 1-DL-MTRP and killed at 96 hours post-ROSC. Pure Link RNA Mini Kit (Ambion, Carlsbad, CA USA) was used in according to the manufacturer's instructions. Samples of total RNA (300 ng) were treated with DNAse (Applied Biosystems, Foster City, CA, USA) and reverse-transcribed with random hexamer primers using multiscribe reverse transcriptase (TaqMan reverse transcription reagents, Applied Biosystems, Foster City, CA, USA). The same starting concentrations of cDNA template were used in all cases. Real-time PCR was performed using Power SYBR Green according to the manufacturer's instructions (Applied Biosystems). *Glyceraldehyde 3-phosphate dehydrogenase* (*Gapdh)* was used as the reference gene, and the relative gene expression levels were determined according to the ΔΔCt method (Applied Biosystems). Data are presented as fold change compared with control group. Primer sets were designed to span exon junctions (https://www.ncbi.nlm.nih.gov/tools/primer-blast/) in order to amplify only spliced RNA. GeneBank accession: ***Gapdh***: NM_017008.4. **Interleukin 1 beta** (*IL1β)*: NM_031512.2. ***Arginase 1*** (*Arg1)*: NM_017134.3. The primer sequences were as follows: ***Gapdh*** forward (fwd): ccgcatcttcttgtgcagtg and reverse (rev): cgatacggccaaatccgttc. ***IL1β*** fwd: gctatggcaactgtccctga and rev: aagggcttggaagcaatcctta. ***Arg1*** fwd: tttctctaagggacagcctcg and rev cagatccccgtggtctctca.

Table S1. Hemodynamics in CA/CPR rats. Hemodynamics were monitored invasively during the 2 hours observation. All data are reported as mean ± SD when normally distributed, median [Q1-Q3] when non-normally distributed of 23 rats. Data were analysed by one-way RM ANOVA with Tukey's multiple comparisons test or Kruskal-Wallis test with Dunn's multiple comparisons test, ***P<0.001 vs pre-CA.

Heart rate (HR), beats/min	
Pre-CA	391 ± 37
PR 10 min	293 ± 72 ***
PR 1 h	378 ± 30
PR 2 h	389 ± 28
Systolic arterial pressure (SAP), mmHg	
Pre-CA	158 ± 14
PR 10 min	101 ± 16 ***
PR 1 h	99 ± 22 ***
PR 2 h	114 ± 27 ***
Diastolic arterial pressure (DAP), mmHg	
Pre-CA	115 ± 17
PR 10 min	61 ± 19 ***
PR 1 h	69 ± 23 ***
PR 2 h	78 ± 26 ***
Mean arterial pressure (MAP), mmHg	
Pre-CA	135 ± 17
PR 10 min	76 ± 18 ***
PR 1 h	80 ± 24 ***

PR 2 h	92 ± 28 ***
Coronary perfusion pressure (CPP), mmHg	
Pre-CA	112 ± 18
PR 10 min	58 ± 19 ***
PR 1 h	66 ± 23 ***
PR 2 h	74 ± 26 ***
High-sensitivity cardiac troponin T, pg/L	
Pre-CA	54 [37-144]
PR 10 min	701 [618- 1057] ***
PR 2 h	4066 [3101- 5104] ***

Table S2. TRP and KP metabolites in hippocampus in *naïve* and *sham* rats. Hippocampal **c**oncentrations of Tryptophan (TRP), Kynurenine (KYN), Kynurenic acid (KYNA), 3-hydroxyanthranilic acid (3-HAA) and the KYN/TRP ratio in naïve (n=4) and sham (n=5) rats. Data are reported as median with [Q1-Q3]. The effect of surgery (*naïve* vs. *sham*) were analysed by Mann-Whitney U test.

	***Naïve* rats**	***Sham* rats**	***P*-value**
TRP, µg/mL	4.83 [4.74 - 5.12]	5.07 [5.05 - 5.30]	0.1456
KYN, µg /mL	42.3 [40.6 - 71.5]	64.8 [53.0 – 77.5]	0.3825
KYN/TRP ratio	0.009 [0.008 - 0.015]	0.012 [0.010 - 0.015]	0.5087
KYNA, ng/mL	2.30 [1.79 – 6.01]	2.48 [2.36 – 3.16]	0.5742
3-HAA, ng/mL	0.233 [0.175 - 0.263]	0.200 [0.177 - 0.236]	0.6519

Table S3. Basal levels of KP metabolites in plasma. Concentrations of Tryptophan (TRP), Kynurenine (KYN) and the KYN/TRP ratio in plasma 15 min before CA (pre-CA) in rats treated with vehicle (n=15) or two doses of 800 mg/kg 1-DL-MTRP given by gavage 16h and 2h before CA (n=13) (referring to Figure 2 in the main text). Data are reported as median with [Q1-Q3] and were analysed by *t*-test with Welch's correction for unpaired measurements: $^{+}P<0.05$ and $^{++}P<0.05$ versus vehicle.

	Vehicle – pre-CA	**1-DL-MTRP – pre-CA**	***P*-value**
TRP, µg/mL	11.14 [9.57 – 14.36]	13.03 [12.25 – 18.69]	0.0312 $^{+}$
KYN, µg /mL	0.350 [0.267 – 0.377]	0.248 [0.203 – 0.288]	0.0243 $^{+}$
KYN/TRP ratio	0.027 [0.020 - 0.041]	0.017 [0.012 - 0.023]	0.0056 $^{++}$

Table S4. Endogenous levels of KP metabolites in *naïve* rats. Concentrations of hippocampal Tryptophan (TRP), Kynurenine (KYN) and the KYN/TRP ratio in naïve rats (n=6) analysed in the two independent experimental sessions (n=3 rats per session, as described in the text) and used to normalize the values in vehicle- and 1-DL-MTRP-treated rats.

Variable	**Experimental session 1** **Mean ± SD**	**Experimental session 2** **Mean ± SD**
TRP, µg/g	3.34 ± 0.38	5.75 ± 0.39
KYN, µg/g	0.067 ± 0.033	0.030 ± 0.001
KYN/TRP ratio	0.0197 ± 0.0084	0.0053 ± 0.0004
5-HT, µg/g	0.286 ± 0.021	0.428 ± 0.159

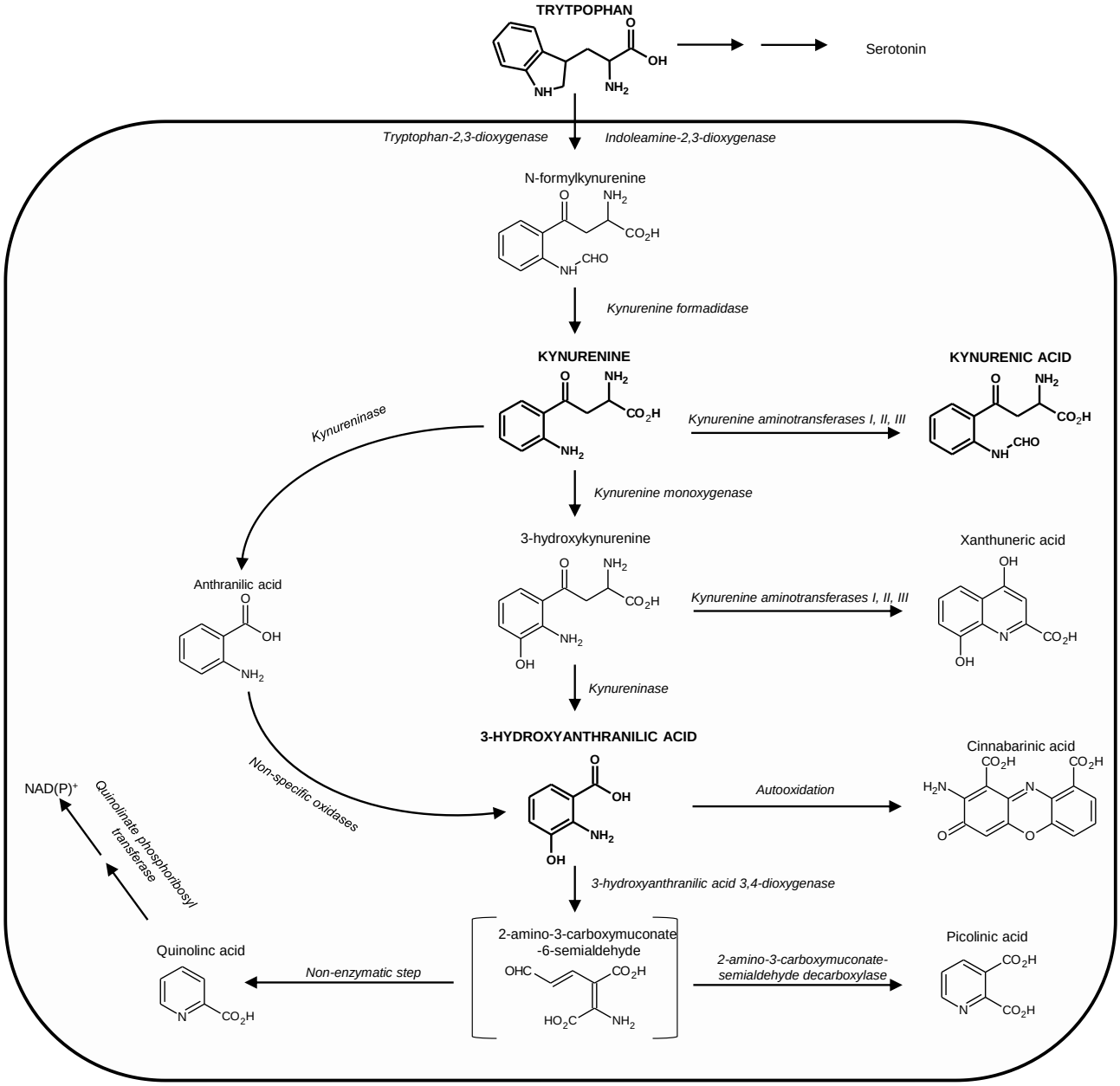

Figure S1. Overview of the kynurenine pathway (highlighted inside the box). Metabolites considered in this study are in upper case. Enzymes involved in kynurenine pathway are in italics.

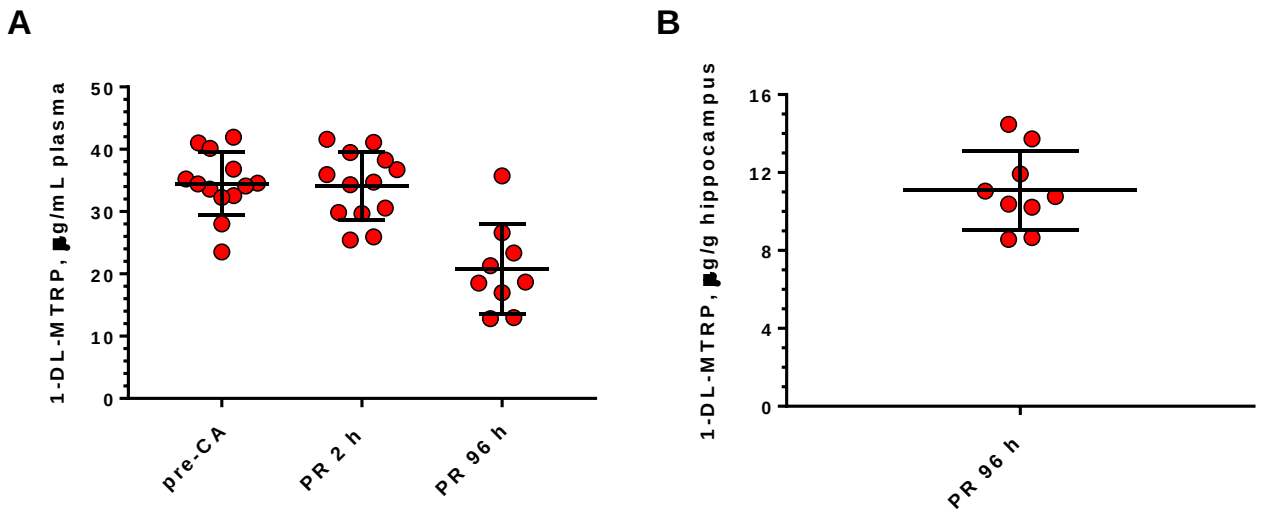

Figure S2. Aim #2: 1-DL-MTRP levels in plasma and hippocampus. (A) Plasma and **(B)** hippocampal levels of 1-DL-MTRP in rats pre-treated with the IDO inhibitor with two doses of 800 mg/kg given by gavage 16 hours and 2 hours before CA. Serial plasma samples were obtained 15 min before CA (pre-CA), 2 hours (PR 2 h) and 96 hours (PR 96 h) post-ROSC. Hippocampal analyses were done at euthanasia 96 hours post-ROSC. Data are reported as means ± SD.

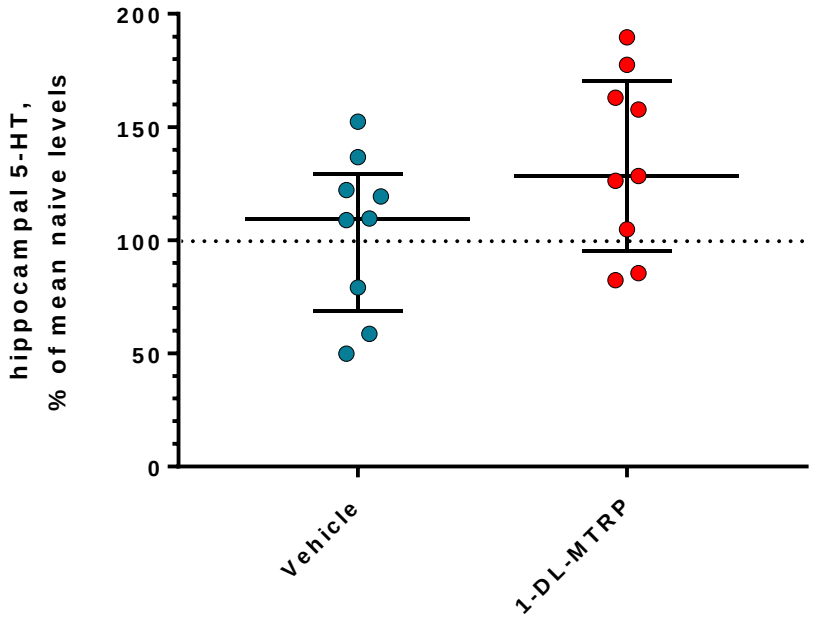

Figure S3 - Effect of IDO inhibition on 5-HT in hippocampus. Concentrations of 5-HT and 5-HT/KYN ratio measured in hippocampus 96 hours post-ROSC (PR 96 h) in rats treated with vehicle (*n* = 9) or two doses of 800 mg/kg 1-DL-MTRP given by gavage 16 h and 2h before CA (*n* = 9). Since this experiment included two independent sessions, each of them including three naïve rats, for each session we normalized the values of 5-HT measured in vehicle- and 1-DL-MTRP-treated rats to the mean values obtained in the corresponding naïve rats (absolute levels are reported in Table S4). Individual points are reported with median and [Q1-Q3] Data were analysed by Kruskal-Wallis test followed by Dunn's multi-comparison test.

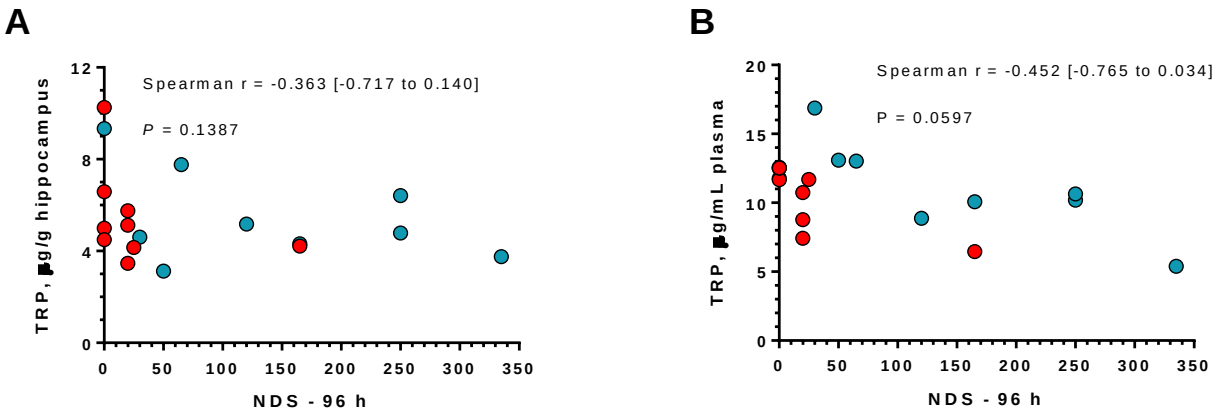

Figure S4. Correlation analysis between tryptophan (TRP) levels (plasma and hippocampus) and neurological deficit score (NDS) at 96 hours post-ROSC.

Correlations between NDS and **(A)** hippocampal and **(B)** plasma levels of TRP 96 hours post-ROSC in rats treated with vehicle (teal blue circles, n=9) or 1-DL-MTRP (800 mg/kg/dose) (red circles, n=9) given by gavage 16 and 2 hours before CA. Correlations were calculated with Spearman's method: rank correlation coefficient *r* [95% CI] and *P*-value (two-tailed) of the correlation are indicated inside the figures. $P<0.05$ was considered significant.

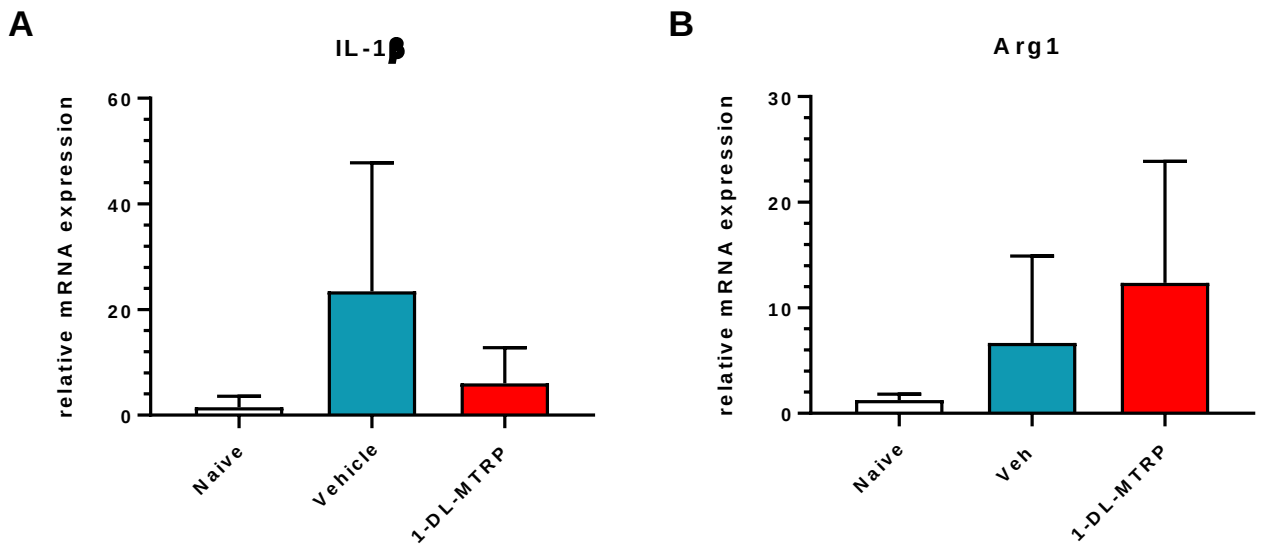

Figure S5. Cortical mRNA expression of pro- and anti-inflammatory genes 96 hours post-ROSC. Relative gene expression analysis of (A) Interleukin 1 beta (IL1β) and (A) Arginase 1 (Arg1) in the brain cortex of naïve rats, and in vehicle- and 1-DL-MTRP –treated rats 96 hours post-ROSC (n=4-6/group). Data were analyzed by Kruskal-Wallis test followed by Dunn's multi-comparison test. Data are expressed as fold induction and reported as mean ± SD.